BNL 36327

DETAILED DESCRIPTION AND PERFORMANCE OF A PASSIVE PERFLUOROCARBON TRACER SYSTEM FOR BUILDING VENTILATION AND AIR EXCHANGE MEASUREMENTS

Russell N. Dietz, Robert W. Goodrich, Edgar A. Cote, and
Robert F. Wieser

February 1985

Presented at the
Symposium on Measured Air Leakage Performance of Buildings,
American Society for Testing and Materials,
Philadelphia, PA
April 2-3, 1984

DEPARTMENT OF APPLIED SCIENCE

BROOKHAVEN NATIONAL LABORATORY
UPTON, LONG ISLAND, NEW YORK 11973

BNL 36327

DETAILED DESCRIPTION AND PERFORMANCE OF A PASSIVE PERFLUOROCARBON TRACER SYSTEM FOR BUILDING VENTILATION AND AIR EXCHANGE MEASUREMENTS

by

Russell N. Dietz, Robert W. Goodrich,
Edgar A. Cote, and Robert F. Wieser

Environmental Chemistry Division
Department of Applied Science
Brookhaven National Laboratory
Upton, NY 11973

February 1985

Presented at the
Symposium on Measured Air Leakage
Performance of Buildings,
American Society for Testing and Materials
Philadelphia, PA
April 2-3, 1984

This research was performed under the auspices of the United States
Department of Energy under Contract No. DE-AC02-76CH00016

ABSTRACT

The manufacturing procedures and performance of a building air infiltration kit consisting of miniature passive perfluorocarbon tracer (PFT) permeation sources and passive adsorption tube samplers are described. Having four PFT-types available, homes and buildings with up to four separate zones can be fully evaluated under steady state conditions for the air infiltration and exfiltration rates from each zone as well as the air exchange rates between zones using this inexpensive and non-obtrusive field kit. Complete details on deployment in homes and on gas chromatographic analysis of the passive samplers are presented. Examples of total air changes per hour (ACH) results in several studies showed average values between 0.25 to 0.64 h^{-1}. A generalized correlation was used to characterize the leakiness of eleven homes in the U.S. and Canada, showing ACH dependency only on inside-outside temperature difference, wind speed to the 1.5 power, and a subjective terrain factor; the approach has application in evaluating weatherization performance. Details of multizone measurements in four homes provided insight into the role of attics, crawl-spaces, and basements on the indoor air quality and weatherization needs for the living zone.

KEY WORDS: Air infiltration, perfluorocarbon tracers, passive sampler, multizone modeling, gas chromatograph, air leakage, weatherization, indoor air quality

INTRODUCTION

During the last decade, concern for the quality of indoor air has increased, in main motivated by the energy conservation and alternative fuel practices now employed in many homes [1], but also from increased recognition of the fact that individuals spend the greatest portion of their lives within the indoor environment. These energy cost reduction practices will continue to be implemented in both the private and commercial sector, in part further motivated by some limitations in the energy supply side in certain locations.

Since about one-third of the heat loss in homes during the heating season is attributable to air exfiltration, the escape of heated air and its replacement by cold infiltrating air, attempts to reduce that loss may increase the occupant's exposure to internally generated pollutants. In many commercial, public, and industrial buildings (e.g., hospitals, office buildings, etc.), not only is there a concern for the extent of total air infiltration but also for the distribution of that ventilation within the many floors of naturally ventilated buildings or between the heating, ventilating, and air conditioning (HVAC) zones of building equipped with such systems.

To quantify the extent of air infiltration in buildings, one of two techniques have generally been used, either the conservative tracer approach or a building pressurization technique; a review of both methods is provided elsewhere [2]. Briefly, the tracer approach determines the infiltration rate as it normally exists in the building by either measuring the decay of the tracer concentration (if only an initial quantity is injected) or its steady state concentration (if a continuous known tracer release rate is used) and calculating the steady state infiltration rate from a simple material balance model [3]. The pressurization method requires a blower assembly to be installed and the total flow rate developed by the blower when the house or small building is brought to a specified pressure is related to the expected normal exfiltration rate through the use of a complex empirical model [4]. This latter method was never intended for larger, more complex buildings and now it is generally being conceded that even for the case of small, single zone homes, the pressurization method is not giving a reliable measure of the air exfiltration rate under normal conditions.

Although tracer techniques provide the most reliable approach to determining air infiltration rates and rates of air exchange between zones in buildings, most methods either have been costly to field implement or have provided only brief (1 to 4h) measures of the rates. Because of the need for a simple, yet reliable tracer technique, a kit was developed coined the Brookhaven National Laboratory Air Infiltration Measurement System (BNL/AIMS). The field components, miniature perfluorocarbon tracer (PFT) permeation sources and passive samplers, are quite inexpensive and reusable, require no trained field personnel, and can provide integrated measurements over days or months [1,5]. With the use of a programmable multi-tube sampler or a portable real-time analyzer, short-term (e.g., hourly) variations can also be determined.

The BNL/AIMS is based on the applicable steady state assumption for a home considered as a single, well-mixed zone such that the average tracer concentration in that home is equal to the emission rate of the tracer source divided by the air exfiltration rate. Knowing the source rate and by measuring the average concentration with the passive sampler, a means to calculate the approximate average air exfiltration rate is thereby established. Extending this technique to a multichamber concept, in which a different type of PFT source is deployed in each chamber of a building, allows the calculation of not only the infiltration rates in each chamber but also the air exchange rates between chambers as well. Since both the PFT source and the passive sampler, a miniature Capillary Adsorption Tube Sampler (CATS), are about the size of a cigarette, inexpensive, and reusable, the BNL/AIMS is a very cost-effective means (if not the only means) for determining these air exchange rates.

BNL/AIMS makes use of the Brookhaven PFT measurement capability that has been under development and applied to long range atmospheric tracing for the past 7 years [6,7]. The technology for the sampling and analysis of PFTs is well established and for long range atmospheric tracing, PFTs have supplanted the use of SF_6, sulfur hexafluoride [7].

This paper provides the necessary details for other potential users to duplicate the system which consists of field components (the miniature PFT sources and passive samplers) and a laboratory component (an electron capture gas chromatographic analyzer). Some intercomparisons with other researchers' methods are presented as well as some results from field use in homes. A simple model is presented for applying the technique in two and three zone cases, which are demonstrated. Some results of the effect of wind speed and inside-outside air temperature differences on the whole house air exfiltration rate are also presented.

EXPERIMENTAL

In this section, the details on the manufacture, testing, and calibration of the PFT sources and passive samplers will be provided as well as the scheme for the gas chromatographic analysis of the samplers when they are returned for the laboratory.

The Tracer Source

Fully fluorinated organic compounds of the perfluoroalkylcycloalkane (PACA) family were chosen as the class of PFTs because they have a high electron capture detector (ECD) response (nearly comparable to that of SF_6), a very low atmospheric background (cf. Table 1; SF_6 background is about 900 fL/L), are harmless to health and the environment [7,8], are modest in cost (about $100/kg), and have extreme chemical stability. This characteristic is very necessary since the analysis scheme includes chemical processing of the recovered constituents from the air samples in order to destroy and remove ECD-sensitive interfering components, such as ambient chlorofluorocarbons, which are present in the air at concentrations orders of magnitude higher than that of the PFT.

The PFT source is a small permeation device which, at a known temperature, emits a constant rate of PFT vapor through a silicone rubber plug connected to a source of the PFT liquid. Aluminum shells (E.I. duPont and Co., Inc., Wilmington, Del., No. S-140) 32-mm (1.25-in.) long by 6.6-mm (0.26-in.) ID, are flared slightly to facilitate the insertion of the oversized silicone rubber plugs. The shells are then lightly lubricated (swabbed with a solution of 5% silicone grease in ethylacetate) and air dried in an inverted position to concentrate the grease near the openings.

A code number is engraved onto the aluminum shells for identification of the PFT source, silicone rubber plug type, and the number of the source.

Placed upright into a small holder, about 20 of the shells are filled in succession with exactly 0.4 mL (1000 L = 1 m^3) of the appropriate PFT liquid using an automatic pipette (SMI/G, micropipettor). Table 1 lists the presently used PFTs, which are all liquids at room temperature (boiling points from 45° to 102°C); with 4 PFT types, a building with as many as 4 zones can be characterized (see Theory section). The pre-cut plugs, 12.7-mm (0.5 in.) long by 7-mm (0.275 in.) OD, are inserted, pressed flush to the end, and crimped (duPont, Pompton Lakes, N.J., Lab Model Crimper) into the shell. Both the aluminum shells and the crimper were previously used in an electric blasting cap tagging program [8]. About 500 sources can be made per person-week. Fig. 1 gives a schematic diagram of a typical source.

A subset of about 1 PFT source for every 50 made is kept in a constant (25°) temperature chamber and periodically (e.g., monthly) weighed on a high precision balance to determine the rate of emission. Using the gas law constant and the molecular weight, the gravimetric rate can be converted to a volumetric rate which can be compared to that determined chromatographically when a source is placed in a known flow rate of air (at a known temperature) and the PFT concentration measured on a calibrated gas chromatograph.

The extent of the effect of temperature on the PFT source rate is determined by measuring the volumetric rate chromatographically when the source temperature is varied from 25° to 37°C. In addition, several sources were placed in a 37°C oven for gravimetric determination of the effect of temperature as well.

A word of caution. As will be shown, the concentrations to be measured in homes and buildings are quite low, typically only a few parts per trillion. Thus, it is very important to keep the PFT containers, any source preparation, and the sources themselves well separated (i.e., in ventilated hoods or a separate building) from any sampling and analysis equipment.

The Tracer Samplers

Two types of PFT samplers have been used, a passive sampler designed and fabricated at Brookhaven and a programmable sampler, conceived at Brookhaven, but now commercially available. The former will be described in detail, but the latter will only be briefly mentioned because it can be purchased.

Passive Sampler - Originally coined the Capillary Adsorption Tube Sampler (CATS) because of a capillary tube on one end [2], the present configuration is shown in Fig. 2. A glass tube, 6.4-mm (0.25-in.) OD by 4-mm (0.156-in.) ID by 6.4-cm (2.5-in.) long, with a 45° taper ground at the ends to about 1/3 the wall thickness (to prevent cutting of O-rings in the desorption apparatus) is cut from conventional pyrex glass tubing selected to have an ID within ±1.5% of the design value; the length is cut to within ±0.8 mm. This tolerance is necessary to keep the sampling rate, which is proportional to the cross-sectional area and inversely proportional to the length from the mouth of the glass tube to the surface of the adsorbent bed, within ±3% precision [2].

Screens to retain the adsorbent material are fabricated by punching 9.5 mm (3/8-in.) OD discs from 150 mesh stainless steel wire cloth (Newark Wire Cloth, Newark, N.J.,) and then shaping into a cup by pressing the disc through a 4.1 mm (0.16-in.) hole in a 8-mm thick brass plate with the back of a 3.6 mm (No. 28) drill bit mounted in a drill press. The screen cups are then washed in a degreasing solvent, detergent, and finally distilled water in an ultrasonic bath.

The charcoal-like adsorbent, Ambersorb (Type 347, Rohm and Haas, Inc., Philadelphia, Pa.) is boiled in distilled water 3 times, decanting away any fine dust floating on the surface. Next, since the adsorbent is in the form of small beads, the material is dried and then rolled down a very shallow inclined plane to separate any shapes that are not nearly perfect spheres (much of this non-spherical material was found to be compacted particles of Ambersorb dust). Finally, it is boiled again until the decanted fluid is clear, dried, and sieved to a 30 to 50 mesh size. Coconut charcoal, which can be used in place of Ambersorb, is treated in the same way but excluding rolling.

Once the glass tubes have been cleaned using detergent solution and an identification number has been either hand-engraved using a diamond-tipped vibrator (Acme Burgess, Grayslake, Ill., Model 74) or fired into the glass using powdered lead glass black numbered decals (Whale Apparatus Co., Hellertown, Pa.), a cupped screen is then pressed into one end of the tube to a depth of 2.75 cm. Then the glass tube is filled with 64 mg of the prepared adsorbent and a screen placed in the other end. A small cup holding exactly 64 mg (0.11 cm^3) is used for rapid filling of the tubes.

Whether for initial bakeout or for thermal desorption and recovery of sampled PFTs, a special rack with 23 positions was built as shown in Fig. 3. The nichrome heating wire element consists of about 10 turns of 0.8-mm OD (20 gauge) nichrome wire (approx. 23-cm length) such that 4.2 VAC (~8.5 amps or 36 watts) heats the CATS tube to 450°C in 0.5 min and 1.9 VAC (~3.8 amps or 7 watts) holds that temperature for another 0.5 min to effect the sample recovery; power is supplied from a transformer with a secondary rated at 6.3 VAC and 10 amps (Essex/Stancor No. P-6308). The tubes are placed into the rack by slipping through the heating coil (with one rack end removed) until they contact the spring-loaded O-ring seal pistons; the removal end, 25-mm (1-in.) Al square stock, is replaced and the eccentric cam compresses the tube ends against the spring-loaded seals. The open 1.59-mm (1/16-in.) tubing ends are connected to a 24-position Scanivalve rotary valve assembly (Gilian Instrument Corp., Wayne, N.J.) which has an electrical rotary switch to bring the desorption power to the proper tube.

An alternatively designed desorption rack has different tube seals. A double O-ring seal is accomplished by the tube slipping through two O-rings, 9.5-mm (0.375-in.) OD by 6.4-mm (0.25-in.) ID, trapped in each end of the aluminum square stock; other aspects remain the same.

After initial fabrication of the CATS passive sampler, it is made ready for its first use by flushing with distilled water and then thermally desorbing at 425° to 450°C for about 20 min. The ends are then sealed with specially fabricated polyurethane rubber caps (Girard Rubber Co., Elmsford, N.Y., U103B-PU).

Sampling commences when the rubber cap near the numbered end is removed. Since the rate of sampling is proportional to the tracer diffusivity in air, the theoretical effective air sampling rates for each tracer are 214 mL/day for PDCB and PMCP; 201 for PMCH; and 188 for PDCH [2]. Rates are confirmed with standards and simultaneous programmable sampler measurements.

Programmable Sampler - The commercially available sampler (Gilian Instrument Corp., Model RD113) contains a lid and a base assembly, which together weigh just 7 Kg. The lid assembly contains 23 stainless steel sampling tubes, 3.2-mm (0.125-in.) OD by 0.15-mm (0.006-in.) wall by 15.2-cm (6-in.) long, filled in the center with 150 mg of the Ambersorb adsorbent. Connected to a common inlet and outlet through the same Scanivalve rotary valve assembly used for the CATS desorption rack, each tube adsorbs all the PFTs in the air pulled through them at a rate, duration, and start time controlled by the pump, 7-day calendar clock, and battery all housed in the base assembly. Thermal desorption for recovery of the sample back in the laboratory occurs by direct ohmic heating of the sampling tubes. A low voltage, high current (1.3 VAC at about 15 amps) is passed directly through the wall of the stainless steel tube which attains a temperature of over 400°C. This unit, coined the Brookhaven Atmospheric Tracer Sampler (BATS), has been used in many atmospheric and home infiltration tests [2,6,7].

The Laboratory Gas Chromatographic Analyzer

The determination of PFTs collected via either the passive or programmable samplers is accomplished with a gas chromatograph (GC) system (Varian Instrument Corp., Floral Park, N.J., Model 3700 GC with a Model CDS-111 integrator-controller) modified at Brookhaven. The scheme includes thermal desorption, chemical and physical processing, chromatographic separation, and electron capture detector (ECD) determination of the quantity of tracer recovered. Because the analysis system is unique and necessary, a detailed description will be presented here.

First a brief description will be given and then a more detailed accounting with reference to the schematic diagram and the sequencing of events. Before the sample is thermally desorbed, the sampler tube is purged with carrier gas (5% H_2 in N_2) for a short period of time to remove any traces of oxygen which otherwise would react with the PFTs during the 400°C desorption recovery. The sample is purged through the precut catalyst (cf. Table 2), the dryer to remove water vapor, and the two precut columns before entering an adsorbent trap. The 10-cm long catalyst bed in the presence of the hydrogen in the carrier gas reduces any chlorofluorocarbon compounds, as well as any remaining oxygen to their hydrogenated forms, thus rendering these interfering compounds non-electron-capturing. After the surviving PFTs elute from the precut column, heavier molecular weight constitutents still within the column are purged to the atmosphere by reversing the direction of flow. Meanwhile, the eluted PFTs are re-concentrated within a 10-cm long Porapak QS adsorbent trap.

The purpose of the QS trap on the GC is two-fold. First, by not opening the trap until the first PFT eluting from the pre-cut column arrives, some lighter constituents are discarded. Second, after the precut column is backflushed, the trap remains open for 1 min to further purge away light-interfering gases, and then is closed. When the Porapak QS trap has been heated to 200°C and opened, the PFTs are flushed through the main catalyst (cf. Table 2) for final clean-up before entering the main column for separation of the PFTs prior to detection in the ECD. While this is occurring, the next sample tube can be thermally desorbed and loaded onto the QS trap once it has sufficiently cooled (about 50°C), thus almost halving the overall PFT sample recovery and analysis time by overlapping the stages. Automation of the sequential analysis of all 23 tubes in either a CATS desorption rack or a BATS lid is accomplished by using the BATS base timing capability to initiate the GC timing sequence as each new tube steps in place. Each analysis, including reporting of the peak areas, takes 10 min; 23 tubes are analyzed in just under 4 hours.

Fig. 4 shows the detailed plumbing and valving used to effect the automated chemical and physical processing during the analysis of the PFT samples. Automation occurs through the use of 8 external events contained within the CDS-111. As shown in the footnote of Table 3, 1 event starts and stops the recorder paper, 4 events operate the 4 valves, and 3 events control the heating of the sampler tube and the Porapak QS trap. Three 6-port (Valco Instrument Co., Houston, Tex., SSAC6T Shaft Seal) and one 4-port (Valco SSAC4UT Shaft Seal) valves with air operators are used. Vespel cone seals are preferred to the Teflon filled ceramic type because the latter have been found to bleed contaminants at temperatures above 100°C. With the exception of the sample valve, they are mounted within the GC oven.

The heating events operate through optically isolated solid state relays such that at specified times the desorption power can be turned on (code .10), and the power (approximately 110 VAC) is then available at its full (High) value (code .12) or at a reduced (Low) level through a solid state rheostat (code .13) to be diverted to both the primary of a specially wound QS-BATS transformer (capable of supplying 1.3 VAC at 15 amps) which is located in the GC and, through a CATS-rack relay, to the primary of the CATS transformer previously described. The third heating event is used both to direct the secondary of the QS-BATS transformer to heat either the Porapak QS trap (code .14) or the BATS sample tube (code .15) and to activate the CATS-rack relay which brings the high-low voltage to the primary of the CATS transformer when CATS tubes are analyzed in place of BATS tubes.

The events sequence for a typical analysis is shown in Table 3. Whether CATS or BATS are being analyzed, the BATS base is set for a 10-min sample duration and a value equal to the number of tubes to be analyzed plus 1 is entered into the sample quantity and the unit is turned on. When a tube is stepped into position, a signal is sent to the CDS-111 to start the event times as listed in Table 3. At zero time, all the valves are in the "off" position, 90° counterclockwise to the position shown in Fig. 4. This allows clean carrier gas from needle valve 3, which flows through the shell side of the permeation dryer at about 15 ml/min, to flow into port 1 of the sample valve (V_1), out port 3 to flush the air out of the sample tube, into port 4, and out port 2 to the vent. Also the flow controller maintains 20 ml/min into port 4 of the flow direction valve (V_3), out port 2 to port 1 of the QS valve (V_4), which is also isolating the Porapak QS trap, out port 3 to port 5 of V_3, out port 6 to the main catalyst located in injector oven A, through the main column and on into the ECD. At the same time, the panel regulator supplies gas at 25 ml/min to port 2 of the precut valve (V_2), out port 4 and backflushes the precut column, the dryer, and the precut catalyst located in injector oven B to port 5 of V_1, out port 6 to port 1 of V_2, out port 3 and finally to needle valve 5 and vented; thus any heavy constituents from the previous analysis are being flushed away.

As the event sequence continues, the recorder starts and high power is applied to the QS trap to rapidly heat it to 200°C; at 0.35 min the heat switches to low power to maintain that temperature and at 0.50 min the previous sample collected in the trap is injected into the main column for analysis. At 1.60 min, the trap is isolated and begins cooling; also the heating selector is switched to the sampler tube position (but is not turned on). The flow direction valve (V_3) is turned on at 2.30 min, a time which occurs between the elution of peaks of interest, such that gas from the flow controller, entering port 4 and leaving port 6, goes directly to the main catalyst and column, thus isolating that part of the system from the operation of other valves. Then at about 5 min, the precut and sample valves (V_2 and V_1, respectively) are turned on and the BATS or CATS sample tube is heated to 400° to 425°C. In this position, carrier gas enters port 2 of V_2, out port 1 to port 6 of V_1, out port 4, flushing the desorbed constituents from the sample tube into port 3, out port 5 through the precut catalyst, dryer and precut column, into port 4 of V_2 and out port 6, into port 3 of V_3 and out port 5, into port 3 of V_4 (which is in the off position) and out port 1 (thereby temporarily by-passing the QS trap), into port 2 of V_3 and out port 1 to vent. Thus until V_4 is turned on at 5.70 min, the early eluting constituents, those that are not wanted, are not trapped; from that time and until 7.60 min the QS trap is collecting all the constituents desired. Immediately thereafter all the other valves are turned off so that any heavy constituents still in the precut column are backflushed to vent.

When the recorder shuts off at 8.01 min, the analysis is complete and the report of the peak areas, which is proportional to the quantity of each tracer, is printed as well as transmitted to a magnetic tape, which can then be processed on a Tektronic 4052 desk top computer. The GC is ready for the repeat of the cycle on a 10-min frequency.

Gas standards for calibrating the GC were prepared in the concentration range from 1 to 10,000 pL/L by first preparing 1000 ppm primary standards in He either gravimetrically or volumetrically and verifying on a thermal conductivity GC which was calibrated with pure PFT vapors. These primary standards were then successively diluted with ultra pure air (Scientific Gas Products, Plain field, N.J.) in Spectra-Seal aluminum cylinders (Airco

Industrial Gases, Riverton, N.J.). Regular steel cylinders were found to adsorb significant amounts of the higher boiling point tracers (PMCH and PDCH), especially at concentrations of 1 and 10 pL/L, but the Spectra-Seal cylinders showed no adsorption losses [7].

Calibration of the GC was performed by setting flowrates of 5 and 50 mL/min on the gas cylinder standards and passing the flow through consecutive BATS tubes for different durations. Quantities of from 0.05 to 5000 pL of tracer were then analyzed to calibrate the GC response for each tracer.

THEORY

Numerous researchers have proposed models and methods for using tracer gases in the solution of those models for determining the air infiltration rate into a home or building considered as a single, well-mixed chamber or zone [2,3,9]. Recently, however, it has been recognized that many larger, more complex buildings, especially those with multiple-zoned HVAC systems, and even one-and two-story homes with basements realistically can only best be represented by models which recognize the building as multiple-connected zones, each of which is well mixed [5, 10-12].

In a series of tests, Maldonado demonstrated that the concentration of a tracer was very uniform in conventional, 2.44-m (8-ft) ceiling, rooms such as living rooms, bedrooms, and basements, generally to within ± 1 to 3% [13]. Furthermore, the variations between rooms on the same floor was generally within ± 10%, indicating that an entire floor of a house could be considered as reasonably well-mixed. This had been demonstrated also by

Dietz and Cote [2]. Only between floors was there a significant difference in concentration of as much as 30 to 60%, indicating that different floors should each be considered as separate, well-mixed zones, with finite rates of mixing between those zones. Unusual rooms in the Maldonado test house, such as the greenhouse, which was an open space from the basement level to the second floor, as well as the stairwell, showed evidence of non-uniform mixing in the vertical, i.e., stratification [13].

The consequences of assuming a truly 2- or 3- zone building as a one-zone case can be significant for ventilation, indoor air quality, or energy load assessments. If, for example, a building is comprised of 3 equal-volume zones, each with its own HVAC system, but one is improperly functioning at an air infiltration rate of $0.2h^{-1}$, while the other two are at $1.1h^{-1}$, the overall average considered as a single zone is $0.8h^{-1}$; but the occupants of the first zone might be significantly more uncomfortable than those in either of the other two zones. Similarly, the air quality might be several times poorer in that zone and the heating and cooling loads might be poorly distributed.

In another case, consider a 2-story house with a basement. If it is treated as a single zone, then the concentration of any pollutant from an indoor source would be computed to be the same on all floors. However, because of the stack effect in houses in the winter time, there is generally a net-flow upwards within 2- and 3-level houses [5]. Thus, a pollutant source in the basement (e.g., radon from ground soil), would be highest in the basement and generally half as much or so on the 1st and 2nd floors. For a source on the first floor (e.g., CO from a kitchen range), the concentration would be highest on the 1st floor, somewhat lower on the 2nd floor, but much less in the basement if the stack effect is evident. Finally, from, for example, an artist's studio on the 2nd floor, the paint fumes would be highest on that floor and progressively significantly less on the 1st floor and in the basement.

Although the BNL/AIMS is a powerful technique for simply and inexpensively determining the air exfiltration rate in a single-zone building, its real potential is in application to the determination of air exfiltration rates from each zone and air exchange rates between zones in multi-zoned homes and buildings. The models for one, two, and three-zone cases are presented here.

One-Zone Case

For a building considered as a single, well-mixed zone of known volume, V, containing one type of tracer of known emission rate, $R_s(t)$, such that a tracer concentration, C(t), is measured throughout the house which has an air exfiltration rate of $R_E(t)$, a simple material balance gives

$$V \frac{dC(t)}{dt} = R_s(t) - R_E(t)C(t) \qquad (1)$$

where

V = volume of the building (constant), m^3,

$R_s(t)$= total tracer source rate (variable), nL/h;

$C(t)$ = average tracer concentration in building (variable), $nL/m^3 \equiv pL/L$ and

$R_E(t)$= air exfiltration rate (variable), m^3/h.

Eq 1 is a general solution in which it is assumed that the tracer source rate, the tracer concentration and the exfiltration rate can vary with time; it was also assumed that the tracer concentration in the ambient air, i.e., the infiltrating air, is negligible, which is always the case for PFTs. Eq 1 can then be solved for various modes of tracer experiments including tracer decay, constant concentration, and constant emission rate [2,3].

The PFT sources are designed to provide a constant emission rate source in the building. About 5 to 10 h after deployment, the tracer concentration will become more or less constant, dependent only on slow changes in the exfiltration rate due either to mechanical ventilation or weather changes [2]. For these steady state assumptions (i.e., $dC(t)/dt \approx 0$), Eq 1 becomes

$$\frac{1}{n}\sum_{t=1}^{n}\frac{R_s(t)}{C(t)} = \frac{1}{n}\sum_{t=1}^{n} R_E(t) = R_s\,\frac{1}{n}\sum_{t=1}^{n}\frac{1}{C(t)} \tag{2}$$

assuming that the source rate is constant, i.e., $R_s(t) = R_s$, over $\underline{n}$ periods of concentration. But

$$\begin{aligned}\frac{1}{n}\sum_{t=1}^{n}\frac{1}{C(t)} &= \frac{1}{n}\left(\frac{1}{C(1)}+\frac{1}{C(2)}+\cdots+\frac{1}{C(n)}\right)\\ &= \frac{1}{n}\left(\frac{C(2)C(3)\ldots C(n) + C(1)C(3)\ldots C(n)+\ldots+C(1)C(2)\ldots C(n-1)}{C(1)C(2)\ldots C(n)}\right)\\ &\approx \frac{1}{n}\left(\frac{n\overline{C}^{\,n-1}}{\overline{C}^{\,n}}\right) \approx \frac{1}{\overline{C}}\end{aligned}$$

The second term in Eq 2 is the average infiltration rate, $\overline{R}_E$. Thus,

$$R_E \approx \frac{R_s}{\overline{C}} \tag{3}$$

The approximation in Eq 3 is because it was shown that the reciprocal of an average concentration, $\overline{C}$, which is the quantity that the passive sampler determines, is close to but not identical to the average of reciprocal concentrations. Consider two simple cases in which for each of 5 consecutive intervals of time, a constant concentration truly prevails. As shown in Table 4, assuming a source rate of 1500 nL/h, case 1 assumes a small concentration change (1 nL/m^3) per period and case 2, a larger value (5nL/m^3). The true exfiltration rates for each period are calculated as are the true averages for each case. Lastly, the average R_E calculated from the average concentrations, which are identical in both cases, are computed from Eq 3. As shown in case 1, for small changes in concentration (i.e., exfiltration rate), the true value is very close to that from Eq 3. The difference, less than 1%, is an order of magnitude less than the relative standard deviation of the measurement; thus the results are statistically identical.

For case 2, the calculated exfiltration rate is substantially less than the true average value, by about 27%. But statistically, the two values are identical since this difference is less than either's standard deviation. In addition, if in a real situation the true exfiltration rates varied from 60 to 300 m^3/h, it would appear that an average of 100 is not even substantially different than 137 m^3/h.

Thus, it is concluded that the BNL/AIMS technique, through the use of passive samplers which provide an average tracer concentration, gives a statistically valid indication of the average exfiltration rate, which is a flow rate. To obtain the more common quantity, air changes per unit time, the exfiltration rate must be divided by the volume of the house. For air quality purposes and for energy and material balances, the flow rate is actually a more valuable quantity.

Two-Zone Case

Examples of 2-zone cases are a 2-story house on a slab, a one-story (e.g., ranch) with a basement or a crawl space, and any building which is ventilated with two separate HVAC systems.

Fig. 5 depicts the model for a one-story house (zone 1) with a basement (zone 2). Air can infiltrate from outside the house into each zone (R_{I1} and R_{I2}) and exfiltrate each zone to the outside (R_{E1} and R_{E2}). In addition, air can exchange between the zones in both directions (R_{12} and R_{21}).

Assuming that a different tracer type is used in each zone (tracer 1 in zone 1, etc.), tracer material balances, assuming steady state pertains and there is negligible tracer in the outside air, give the following:

Zone 1

$$R_{21} C_{12} - R_{12} C_{11} - R_{E1} C_{11} = -R_{s1} \tag{4}$$

$$R_{21} C_{22} - R_{21} C_{21} - R_{E1} C_{21} = 0 \tag{5}$$

Zone 2

$$R_{12} C_{11} - R_{21} C_{12} - R_{E2} C_{12} = 0 \tag{6}$$

$$R_{12} C_{21} - R_{21} C_{22} - R_{E2} C_{22} = -R_{s2} \tag{7}$$

where

R_{12}, R_{21} = air exchange rates from zone 1 to 2 and 2 to 1, m^3/h,

R_{E1}, R_{E2} = air exfiltration rates from zones 1 and 2, m^3/h,

R_{s1}, R_{s2} = rates of tracer sources in each respective zone, nL/h, and

C_{11}, C_{21}, C_{12}, C_{22} = concentration of tracer 1 in zone 1, etc., nL/m^3 ($\equiv$ pL/L).

The concentrations are measured with the passive samplers and the tracer source rates are known. Thus, the four unknowns, two air exchange rates and two exfiltration rates, can be solved from the four simultaneous equations. The rate of infiltration for each zone can then be calculated from air mass balances:

$$R_{I1} = R_{E1} + R_{12} - R_{21} \tag{8}$$

$$R_{I2} = R_{E2} + R_{21} - R_{12} \tag{9}$$

The solutions to Eqs 4 to 7 can be obtained by solving as two sets of simultaneous equations, noting that R_{21} can be solved from Eqs 4 and 5 and R_{12} from Eqs 6 and 7. Then R_{E1} and R_{E2} can be obtained from Eqs 5 and 7, respectively. The solutions, which are given in Appendix 1, can also be obtained by any standard matrix inversion routine for use on a desktop computer [14]. This is especially useful when the number of zones increases to 3 or 4.

Once all the flow rates have been determined, simple material balances can then be performed for pollutants in the same building. The following equations

$$R_{21}\ C_{p2} + R_{I1}\ C_{pa} - R_{12}\ C_{p1} - R_{E1}\ C_{p1} = -R_{p1} \tag{10}$$

$$R_{12}\ C_{p1} + R_{I2}\ C_{pa} - R_{21}\ C_{p2} - R_{E2}\ C_{p2} = -R_{p2} \tag{11}$$

where

C_{p1}, C_{p2}, C_{pa} = concentration of pollutant in zone 1, zone 2, and the ambient outside air, respectively,

would then give the pollutant net source strength in each zone of the building. For radon, one would expect a positive term for the basement and a near-zero result for the main floor, since the radon source is generally from soil gas entering a basement [15]. For NO_2 from a gas range, the source term should be positive on the first floor and perhaps negative in the basement, due to scavenging being a dominant mechanism in that zone [16]. Thus, the multi-zone modeling would provide for unique identification and quantification of these processes.

Three-Zone Case

A typical example of a three-zone building is a 2-story house with a basement. Again, assuming that a different tracer source is used in each zone and that the steady state assumption applies, a set of 9 tracer material balance equations can be developed to solve for 9 unknown flow terms (3 exfiltration flow rates, one from each zone, and 6 air exchange rate terms, two leaving each zone). A set of 3 air mass balance equations would provide the 3 unknown infiltration rates.

The solutions to the tracer and air material balance equations are given in Appendix 1. It is apparent that as the number of zones increases, the matrix solution approach with computer assistance is the only manageable way.

N-Zone Case

It is apparent, then, that for N zones, a set of N^2 tracer material balance equations can be written to solve for N^2 unknown flow terms (N exfiltration flow rates, one from each zone, and N(N-1) air exchange rates, i.e., N-1 leaving each zone to flow to another zone). Also, a set of N air mass balance equations would provide the N unknown infiltration rates.

FIELD DEPLOYMENT

In order to avoid contamination, the PFT sources are shipped separately from the passive samplers. When going from house to house during deployment, it is convenient to carry the sources in a container mounted under the hood of the vehicle, i.e., in the engine compartment, which is effectively outside, and the samplers within the vehicle. An alternative would be to place the samplers in a zip-lock plastic bag along with a small satchel of charcoal (e.g., activated coconut or aquarium charcoal) which will keep the concentration of PFT vapor at zero. When a large number of homes are being surveyed, it is generally wise to retain 2 or 3 passive samplers as controls, that is, unopened, in order to verify the absence of contamination during shipment, deployment, and storage.

Since the single and multi-zone models assume that the tracer is well-mixed within each zone, it is desirable to deploy the sources in a manner which provides uniform emission in a zone. Typically, one source is deployed for every 46.5 m^2 (500 ft^2) of living area, in order to establish steady state concentrations of about 10 to 20 pL/L. Thus, in a single story house, e.g., a small ranch house, one source is placed in each extreme end of the house (e.g., the living-dining room area and the master bedroom). In a two-story house, two sources are deployed on the main floor (e.g., the living room and family or dining area) and two upstairs (e.g., the master bedroom and one other bedroom). The doors to all rooms should remain open. If the house has a basement, one or two sources should be deployed in that zone. Ignoring the basement, as will be discussed later, will result in errors in the determination of a pollutant source strength term if it is truly located in the basement.

For a single zone type of measurement, the same type of PFT source should be used on each floor. In houses with basements, the whole house rate may be correctly determined, but the living area infiltration rates and corresponding actual pollutant concentration distributions will not be determinable. For a complete understanding with a multi-zone approach, a different type of tracer should be used on each floor. If a computer system is used to interpret the results, there is essentially no difference in cost with BNL/AIMS to perform a multi-zone measurement compared to a single zone measurement, assuming the same number of sources and samplers are used; thus, the approach selected should be governed by the physical arrangement of the building or house and the subsequent use of the data.

The sources are used as received; they are always emitting tracer, there is nothing to open or uncover, and they may be placed in any orientation. Generally, a PFT source is placed within a meter or so of an outside wall. For example, it can be taped onto the leg of a table or end table or even on a lower portion of a hanging chandelier. Since the source is sensitive to temperature, it should not be placed near a heating or cooling source nor in direct sunlight or other drafty location such as a window. The average temperature of the source must be recorded; the average room temperature gotten from a room thermostat is usually adequate for this purpose, even in the case of one or more daily temperature set-back cycles.

Although it is assumed that the tracer concentration is uniform throughout a zone and thus only one passive sampler need be deployed per zone, it is accepted practice to obtain at least two sample measurements per zone to verify that assumption, if the cost can be justified. The principal cost in this method is, of course, the number of analyses made per home. Thus, the samplers are usually deployed in the same room as the sources but at least 2 to 3 meters from any source and usually near an inside wall location (but at least 0.5 m from any wall, floor or ceiling). They can also be placed on a table or taped to the leg of a chair or table. The samplers have a rubber cap on each end. To initiate sampling, only one cap must be removed (usually the one near the numbered end). The sampler number, location, and time and date sampling commenced must be recorded. At the end of the designated sampling period (e.g., one day, one week, one month, etc.), the sampler is capped and a record made of the time and date sampling ceased. If it is desirable to compute air changes for the house, then the volume of each zone should be recorded.

In large, multi-story multi-zone buildings equipped with HVAC systems, it may be simpler to deploy the appropriate number of sources (e.g., as little as one per 465 m^2, i.e., 5000 ft^2) directly at the entrance to each distribution blower. The air entering the distribution system is in part recycled return air and in part fresh outside air. Thus, in principle, the concentration of tracer in the distribution air is related to the intentional rate of addition of fresh air and should also be identical to the tracer concentration throughout the rooms in that zone. Since the building is further being exchanged with fresh air by natural infiltration, in practice the room tracer concentrations will be less than that in the distribution system. However, the average room tracer concentrations throughout the zones can be used to compute the total exfiltration rate from each zone plus the zone-to-zone air exchange rates. Models are being developed and tested to demonstrate how the PFT method can be used to distinguish natural infiltration from forced ventilation in large buildings and also to determine the efficiency of ventilation systems with respect to stratification.

RESULTS AND DISCUSSION

Before this simple passive tracer source and sampler technique will be accepted widely, the reliability and validity must be documented and comparison of this method with those of previously accepted methods must be presented.

Performance of the Tracer Source

Initial Performance. Usually the sources are fabricated and then set aside for a period of time to allow them to achieve a steady rate of emission. As shown in Fig. 6, the PFT sources are ready for use in just 10 to 12 days after manufacture.

Long-Term Performance. Three of the four tracer types given in Table 1 were fabricated into PFT sources and the gravimetrically determined emission rates determined over two different time periods for silicone rubber plugs of "quoted" 40 (Table 5) and 70 (Table 6) durometer hardness. With the exception of an occasional outlier, the emission rates for each group of 6 sources were comparable to within ±1 to 3%. The rates were determined over a 3-month period at the end of 1982 using an electrobalance and again in the middle of 1983 for a 5-month period with a different balance. The ratio of the rates for the 2 periods was essentially unity, indicating no aging effects.

A larger group of 20 PDCB sources with silicone 60 rubber plugs had the following emission rates for 19 of 20:

Avg.:	47.88 ± 0.93 nL/min (± 1.9%)
Median:	47.93 nL/min
Range:	46.68 to 50.08 nL/min
Outlier:	53.67 nL/min

Although gravimetric calibration is significantly more convenient and in essence more accurate and precise, several sources were also calibrated chromatographically as shown in Table 7. From the standard deviations, it is apparent that the precision of the gravimetric results is at least an order-of-magnitude better than that for GC determinations. The average ratio of gravimetric-to-chromatographic was nearly unity within ± 6%.

Effect of Temperature. Table 8 gives the activation energies found for several PFT sources fabricated with a range of rubber plug hardnesses. The immediate temperature effect measurements were determined over short periods of temperature change (<1 hour) by GC. The long-term temperature effects were determined gravimetrically by placing sources in a 37°C oven and comparing the permeation rate with that found gravimetrically for the same or similar sources when stored in a 25°C oven.

Unfortunately, the quoted hardness of the rubber plugs was not always consistent with the actual hardness as determined by "feel". Thus, the entries into the table are arranged in increasing order of hardness as indicated by decreasing permeation rate, which ranged over less than a factor of two, as did the activation energies (ΔH), for the range in hardnesses covered.

For PDCH, the short-term ΔH ranged from 4 to 7 kcal/mole and 2 to 4 kcal/mole for PDCB. But the long-term ΔH was essentially identical for all three PFTs, having an average value of about 8 ± 1 kcal/mole. The effect of ΔH on the source rate for a 3°C error in the source temperature estimate (the largest anticipated temperature error) is as follows:

ΔH kcal/mole	Rate error for a 3°C temperature error, %
4	7.2
6	11.1
8	15.0
10	19.1

Since all source rates are reported at 25°C, any use at other temperatures must be considered long-term changes. Thus, a 3°C error in temperature is likely to cause a 13 to 16% error in emission rate.

Performance of the Passive Sampler

Tightness of End Caps. When the caps are installed on the sampler (CATS) tube, it is important that the leakage rate be a very small percentage of the normal (one cap removed) sampling rate. This is necessary to prevent contamination with tracers during shipment and storage. As shown in Table 9, the original yellow vinyl cap as well as subsequent Auster black rubber cap had leakage rates of about 0.5 to 0.8%. When a Girard black rubber cap (buna rubber; No. U103B) was used, the rate was 0.06%. Polyurethane rubber tubing had been previously selected for use in the programmable sampler because of its impermeability and lack of solubility towards PFTs, lack of contamination from desorbed rubber constituents, and its excellent clinging or sticking tendency to smooth surfaces. Thus, when the Girard end cap was fashioned from polyurethane (U103B-PU), the leak tightness improved by more than two orders of magnitude to less than 0.0004% of the uncapped rate.

Effect of Temperature and Pressure. Theory states that there is no effect of barometric pressure on the sampling rate and therefore no tests were conducted on that effect.

CATS were exposed to a PMCH/PDCH standard for about 200 min at temperatures of 25°, 35°, and 50°C. As shown in Table 10, the change in the average quantity of tracer sampled for 10°C change in temperature was less than 2%, in agreement with the theoretically expected change; but, within the standard deviation of the measurements, the change was not even discernible. Thus, normal room temperature changes will have no effect on the performance of the passive samplers.

Comparison of CATS with BATS. Eight passive samplers were exposed for 45 min in a chamber containing PDCH during which three BATS tubes were collected. The CATS concentrations averaged 136±5 pL/L and the BATS, 119±2 pL/L. Thus the CATS rate for PDCH was about 14±6% higher than that expected from the dimensions of the passive sampler and an empirically derived diffusion coefficient [2]. Additional tests are being conducted to verify the sampling rates for all 4 PFT types.

Reproducibility of Multiple CATS. As shown in Table 11, the concentrations of 3 PFTs sampled with 20 passive samplers at the same location in a house which contained the three types of tracer sources was quite reproducible to within ±2%. The precision of the analyses can be estimated by ratioing one tracer to another since that ratio is independent of the sampler dimensions (i.e., sampling rate). The last three columns showed that precision to be less than ±1.5%; with the exclusion of 2 out of 20 ratios, the precision was within ±1% for concentration in the 3 to 30 pL/L range.

Gas Chromatograph Performance

Six ambient air samples of about 25-L each, collected with the programmable sampler, were analyzed with the GC system. The chromatograms, two of which are shown in Fig. 7, show the elution of an unknown followed by a small peak representing PDCB, just ahead of a second unknown, which has been identified as ambient PMCP. This is followed by the PMCH peak and then three peaks representing three of the isomers of PDCH. The analysis results of all six samples are shown in Table 12. Since even the PDCB concentration at 0.35 fL/L was determined with ±10% precision with a 25-L sample, typical home concentrations of 3 to 30 pL/L, that is, 4 to 5 orders-of-magnitude higher, could be quantified with just a 2.5-mL air sample. For a passive sampler, that would be equivalent to about a 20-min exposure or sampling period. This accounts for the high analytical precision obtained for the not-quite 2-day sample period results shown in Table 11.

At the 140°C column temperature, Fig. 7 demonstrated that three tracers could be clearly resolved, that is, PDCH, PMCH, and either PMCP or PDCB. In order to better resolve the latter two, the column temperature had to be reduced to about 100°C, at which temperature the PDCH peaks were not entirely eluted until about 28 min. Further research is needed to speed up the analysis time for 4 PFTs. Preliminary tests have shown that by temperature programming the column from 100° to 150°C, starting when the precut column is backflushed, the resolution of four PFTs can be completed in 13 min, including oven cooldown time.

A typical calibration curve for PDCH is shown in Fig. 8. Although the response is supposed to be linear up through nearly the first four orders-of-magnitude, a step or kink occurs at tracer volumes less than 1 pL for this constant current type ECD. The response is supposed to follow the semi-theoretical equation:

$$v = \frac{a\ A}{1 - ab\ A} \tag{12}$$

where

v = the tracer volume, pL

A = integrator area, kilocounts

a,b = product of fundamental rate constants

Eq 12 would apply to an ECD operating in the constant frequency mode or the constant current mode when analyzing weakly electron capturing compounds [17]. For the response shown in Fig. 8, the equation was modified empirically to give

$$v = \frac{a\ A}{1 - ab\ A\,\dfrac{t + A^q}{p + A^q}} \tag{13}$$

where

t,p,q = empirical constants.

Typical values for PMCH are

$a = 0.00266$ $\qquad$ $t = 5.7\text{x}10^6$

$b = 0.000753$ $\qquad$ $p = 6.7\text{x}10^4$

$q = 1.43$

From these values it can be shown that a 0.5% deviation from linearity occurs at just 0.079 pL of PMCH, a 5% deviation at 0.86 pL, and a 25% deviation at 7.4 pL. Thus, typical bi-weekly measurements (about 2.8 L) in a home with tracer concentrations of 3 to 30 pL/L would have collected 8.4 to 84 pL and would be in this error range of more than 25%. Care must be taken to provide accurate calibration over the range of expected tracer quantities.

An ECD working in the constant frequency mode would not suffer from this non-linearity in the early portion of the calibration curve but would have about a 100-fold reduction in dynamic range. This would be inadequate for infiltration-type measurements; the maximum dynamic range of the constant current ECD-mode has been needed on several occasions.

Field Use of BNL/AIMS

The PFT air infiltration measurement system has been deployed in more than 1000 homes with most of the measurements being single or 2-zone types. In this section, examples of that use will be given showing the uniformity of the tracer concentration within a room and on a floor, comparison of the BNL/AIMS versus SF_6 tracer techniques, measurements of infiltration rates from groups of homes in the U.S., Canada, and Sweden, correlation of infiltration rates with meteorological and other parameters, and demonstration of the multizone capability in homes.

Tracer Uniformity in a Room and on a Floor. A number of uses of this technique have demonstrated that the tracer concentration is generally quite uniform within a room and even on the same floor provided doors are not left closed.

Tests were conducted in the Brookhaven House, a passive solar-assisted house with a basement and two floors. As shown in Table 13, two PDCH sources were deployed on the first floor (one in the dining area and one in the family room) and two PMCH on the second floor (one each in the master and bedroom 1). The first two CATS were located side-by-side; the PMCH concentrations were nearly identical (within ± 0.3%) and the PDCH values nearly so (within ± 1.5%). It was noted that the precision of PDCH analyses is typically 5-fold poorer than that for PMCH because the former consists of three broader peaks compared to a single narrow peak for PMCH.

For the five samplers located in the dining-living area, a single large room, the tracer concentrations were quite uniform (within ± 2.6%). For the five on the second floor there was more spread. CATS 584 gave a low PMCH value because there was no source in that room and the door was closed. The average of the other four samplers was within ± 10% for the tracer deployed on that floor. It would appear that as long as bedroom doors are open, two samplers at different locations on the same floor should give a reasonable average of that zone's concentrations.

Subsequently, in September of 1983, with an additional tracer, PDCB, located in the center of the basement, PFT concentration measurements were again made at several locations on each floor as shown in Table 14. Even though the PMCH sources on the second floor were located, one each, in the two bedrooms, the concentration measured in the bathroom off the hall between the two rooms was only slightly less (about 10%) than that found in the bedrooms. This was also true for PDCH on the first floor; the kitchen, which had no source, had an identical concentration to that measured in the other rooms which contained the sources.

Thus, for the open nature of the first floor, the tracer uniformity was exceptionally good, indicating rapid mixing within that floor or zone. For the compartmentalized nature of the second floor, the tracer on that floor was only slightly less well distributed as long as the doors were open (Table 14) but poorly so when a door was closed (Table 13) as expected. It was not apparent why the basement, which was completely open, showed a non-uniformity in the PDCB concentration distribution. Further, it was interesting to note that the PMCH concentration on the first floor was highest in the family room and lowest in the other end, the living room; the staircase to the second floor, where the PMCH sources were deployed, was located in the family room.

The extent of the floor-to-floor mixing can also be inferred from the data in Table 14. Since the PDCB concentrations on the second and first floors were nearly the same and since that tracer source was in the basement, then the rate of air exchange between the first and second floor must be fairly high. The PMCH concentrations were much higher on the first floor compared to the basement and since that tracer source was in the second floor, the air exchange between the basement and first floor is fairly low. Similarly, the PDCH concentrations on the second floor are 4-fold higher than in the basement; hence the air exchange between those floors is quite low.

In conclusion, then, mixing between rooms on the same floor is generally good enough to consider each floor as being well mixed. However, the mixing between floors is much lower, and hence each floor in a house can be considered to be a single, well-mixed, but separate zone in the home. Examples will be given in a later section.

Comparison of BNL/AIMS with Other Techniques. A study was conducted by the Lawrence Berkeley Laboratory (LBL) over the three-week period shown in Table 15. The 480 m^3 house was equipped with an automated SF_6 tracer decay system which measured the infiltration rate every 90 min. During this period, two PDCH sources, one in the living room and one in the basement, and four passive samplers (CATS), two on each floor, were deployed as shown in Table 15. Despite the single source in the living room, the concentration in the bedroom was not substantially less than that in the living room for two reasons: 1) the good mixing that generally occurs on a floor and 2) the presence of a uniform PDCH concentration in the basement which exchanges with the main floor.

Based on the average PDCH concentration of 10.8 ± 1.2 pL/L, the source rate (1632 nL/h), and the volume of the house (481 m^3), the average air infiltration rate of 0.31 h^{-1} was computed, in good agreement wth the 0.33 h^{-1} value obtained from the average of 306 SF_6 decay measurements.

In another study, this one conducted by the University of Wisconsin [18], the BNL/AIMS was deployed in nine homes, for which the average infiltration rate was 0.39 ± 0.22 (cf. Table 16). This result compared very well with the average obtained by a constant SF_6 release technique deployed in eight of the nine homes (0.37 ± 0.21 h^{-1}) . When the SF_6 method was plotted versus the BNL/AIMS, the slope was close to unity (0.82 ± 0.16) with an intercept near zero (0.04 h^{-1}); thus, the methods appear to give very similar results.

Subsequently, the homes were also evaluated with a blower door technique [4], but as shown in Table 16, the infiltration rate was much higher than that from either of the tracer methods. Correlation with the BNL/AIMS showed a very large intercept and the slope had a significantly large standard deviation.

As a result of these two tests, it would appear that the BNL/AIMS gives results in good agreement with the conventional SF_6 techniques, when both are conducted properly, but at significantly reduced costs and manpower requirements. A laboratory chamber validation of BNL/AIMS versus CO_2 tracer decay measurements demonstrated the precision of duplicate sampling (± 1 to 3%) and the ability to accommodate variations in infiltration rates and indoor temperatures in arriving at the correct average ventilation rate by this method [19].

A Sample of Home Air Infiltration Rates. Several groups of homes were evaluated for their air change per hour (ACH) rates using the BNL/AIMS. The frequency distributions for the nine homes in the University of Wisconsin study along with one for seven homes in a Canadian study and another for thirty homes in a Connecticut study are shown in Fig. 9. All were conducted during the February to March 1983 heating period and were generally two-week integrated measurement periods.

The averages for all three sets are quite close, between 0.25 to 0.44 h^{-1}, with two sets being nearly identical, the Wisconsin and Connecticut studies; the seven homes measured in Ottawa, Ontario, were the tightest (0.25 h^{-1}) as they were in a development of energy efficient homes.

Reproducibility of Five Swedish Homes. Five Sparsam models of identical Swedish design were evaluated for air infiltration rate during April 1983; two homes were located in the city of Malmö and three in Stockholm. The two-story design had three bedrooms and a bathroom upstairs and a living room, kitchen, utility room and foyer downstairs.

Four PDCH sources were deployed, two upstairs (bedrooms 2 and 3) and two downstairs (living room and foyer). The four passive samplers were deployed in the same way, two upstairs (bedroom 3 and hall) and two downstairs (living room and foyer). The PDCH concentrations found at each location and the average air changes per hour for the whole house are shown in Table 17.

The two homes in Malmö and two of the three in Stockholm had essentially identical concentration distributions and air infiltration rates, with the latter averaging 0.64 h^{-1} (± 7%) for the four homes and 1.34 h^{-1} for the outlier house, S9. Even the concentrations in the first four homes in the living room, bedroom and hall were nearly identical at 23 pL/L (~ ± 10%) with the foyer higher, 31 pL/L (± 8%), because of the confined space at that location.

This Swedish home design was provided with ventilation ducting to help distribute the passive solar gain and, therefore, is not to be considered typical. Rather, the evaluation shows the consistency of the BNL/AIMS in making air infiltration measurements.

A Generalized Correlation for Parameters Affecting Air Infiltration Rates. It has generally been shown that air infiltration rates are approximately a linear function of the inside-outside temperature difference and also the wind speed; dependence on wind speed, u, has been shown to be between linear (i.e., $u^{1.0}$) and quadratic (i.e., $u^{2.0}$) [20,21]. In this section, correlations of these parameters as well as a terrain factor with infiltration rates will be presented. Since the BNL/AIMS gives integrated average infiltration rates, the temperature and wind data will also be periodically-averaged values.

Studies of an NAHB house over monthly periods from September 1982 to May 1983 are summarized in Table 18. The Conventional Comparison House, an electrically heated house located in Maryland, consisted of a single-story ranch house with a basement that had a sliding door opening to the backyard. The house was located in fairly open terrain, slightly sheltered by other homes nearby. For most of the periods, the measurements were conducted as a two-zone test; the air changes per hour figures are the total house infiltration rates divided by the total house volume.

The cold weather data from October 1982 through February 1983 were correlated successfully as shown in footnote b. of Table 18. The temperature dependence is shown graphically in Fig. 10, in which the ordinate is the air changes per hour (ACH) adjusted for the wind speed, u, effect; the good correlation with Δt is quite apparent. When the temperature effect is subtracted from the ACH and the result is plotted versus wind speed, the data show a reasonably good fit with either $u^{1.5}$ (solid line) or u^2 (dashed line); the 1.5 exponent is preferred based on other experiences.

A generalized correlation, shown in footnote c. of Table 18, has the following form:

$$ACH = L\left(0.006\ \Delta t + \frac{0.03}{c}\ u^{1.5}\right) \tag{14}$$

where

ACH = average air changes per hour or infiltration rate, h^{-1}

L = generalized house leakiness factor ($1<L<5$)

c = terrain sheltering factor ($1<c<10$)

Δt = average inside-outside temperature difference, $^{\circ}C$

u = average wind speed, m/s

Eq 14 was developed from this plus an evaluation of other home infiltration measurements, some of which will follow. The leakiness factor tends to classify a home as to whether it is already reasonably airtight ($L<1$ to 1.5) or is leaky and would benefit from weatherizing corrective action ($L>2.5$ to 3). Similarly, an empirical terrain factor, c, has values for open terrain ($c \approx 1$), moderately sheltered terrain ($c \approx 3$), and highly sheltered terrain ($c \approx 10$).

For the CCH house in Table 18, the leakiness factor, L, was found to be 1.70 ± 0.08 (± 4.7%), indicating a moderately leak-tight home; the terrain factor, c, of 2.3 ± 0.23, was indicative of the slightly sheltered terrain. The calculated infiltration rates were lower in March, April and May than the measured values, presumably from the springtime opening of windows.

Similar studies of the seven Canadian homes discussed earlier were conducted over five measurement periods from mid-February to mid-May 1983. From the seasonal trends of all Apple Hill homes, shown in Fig. 12, it appeared that there were two sets of three houses each that behaved similarly, with the seventh having the highest average infiltration rates. During the three coldest periods, when the infiltration rate dropped from one period to the next for one house, it did so for all seven.

Using the generalized correlation given by Eq 14, the data for all seven homes were used to find the best fit for the leak tightness constant, L, and the terrain factor, c. As shown in Table 19, the correlations for the cold weather gave calculated air change rates within a few percent of the measured rates; in the warmer weather, the calculated rate was usually less than the measured rate as in the NAHB test house.

The L values for three of the houses ranged from 1.3 to 1.5, indicating that they were quite tight; two had values of 1.9 to 2.0; and two had values of about 2.3, indicating that they might benefit from some weather stripping.

The terrain factors, c, ranged from 3 to 21 in Table 19, but the location for all seven homes provided nearly identical terrain, that is, moderately sheltered (c = 3), due to the number of homes in the area. The average c of 13 ± 9 for all seven appears to be high because the average wind speed data reported was quite high and appears to be in error by a factor of 2 to 2.5, based on the average Maryland (Table 18) and Long Island (Table 20) winds, which would have reduced c by 3- to 4-fold to a range of about 1 to 5, consistent with the model.

Three Long Island homes had multizone PFT infiltration measurements conducted from October 1983 to April 1984 on about a semi-monthly basis (the multizone nature of the measurements will be discussed in the next section). As shown in Table 20, the measured ACH were fitted to Eq 14 with an overall average relative standard deviation of ± 9 to ± 12%. The best values for L and c, given in footnote c., indicated that the Dietz and Brookhaven houses were quite tight (L of 1.6 to 1.7) and did not need further weatherizing; the Goodrich house was 3-fold leakier (L of 4.5), indicating a significant weatherization need. The terrain factors determined were representative of the actual siting conditions. The Dietz house was located in a rural development with lightly wooded landscape (c = 2.5); the Brookhaven house, an experimental building, was located in an open area with woods on the north side only (c = 1.9); the Goodrich house, in a more urban setting, was sheltered by homes on both sides and behind (c = 3.0).

The general weatherization correlation represented by Eq 14 would appear to adequately correlate the infiltration rates of homes, requiring only a single measurement period in which ACH, Δt, and u are measured and c is estimated based on the siting status, from c = 1 (flat and open terrain) to c = 10 (very hilly and/or heavily wooded or crowded), to determine an estimate of L, the house leakiness factor. Determining L before and after weatherization would then provide a direct measurement of the effectiveness of the weatherization effort in reducing air infiltration. Two or more measurements before and after weatherization would provide an independent determination of the terrain factor, c. It would appear that this technique should be capable of determining changes in L due to weatherization of greater than about 10 to 15%. The uncertainty can be reduced to about 5 to 10% if the passive samplers from the before and after weatherization periods are analyzed at the same time, thereby eliminating any GC calibration errors.

Based on the seven Canadian, one Maryland, and three Long Island homes, the leakage factor, L, for ten energy efficient homes (i.e., all but the Goodrich house) ranged from a low of 1.27 to a high of 2.28 with an average of 1.77 ± 0.34; excluding the Canadian homes, for which unreasonably high average winds were reported, the average terrain factor, c, was 2.4 ± 0.5 with a range of 1.9 to 3.0, also consistent with the model. Eq 14 also shows that in the winter period (mid-December to mid-March) on Long Island, the temperature difference accounts for 72% of the ACH and wind, 28%, based on a terrain factor, c, of 2.5. During the warmer weather, the correlation always underpredicted the ACH because of opening of windows by the occupants; this was different in the unoccupied Brookhaven house (Table 20). At the extreme, during the summer months, the ACH climbed to 1.5 to 2.0 h^{-1} for the Dietz and Goodrich houses; thus attempts at establishing the weather correlation must be done under consistent physical conditions of doors, windows, vents, etc.

Examples of Multizone Flow Determination in Homes. Applications of the BNL/AIMS technique to the multizone modeling presented earlier provides a simple and convenient way to determine the complete infiltration and air exchange picture for a house [5] or building [22]. In this section, some detailed discussion of the results obtained in 4 houses will be shown for the purposes of demonstrating the capability of the technique and the proper way to deploy sources and samplers for the information desired. This information is that which is sufficient to calculate, for example, pollutant concentrations in different locations within the house for pollutant sources at different locations or heat balances around a home for sizing and zoning the heating system [23].

As an example, for one type of pollutant source in a 3-zone house, material balances around each zone give the following:

$$-(R_{E1}+R_{12}+R_{13})C_{11}+R_{21}C_{12}+R_{31}C_{13}=-R_{s11} \qquad (15)$$

$$R_{12}C_{11}-(R_{E2}+R_{21}+R_{23})C_{12}+R_{32}C_{13}=-R_{s12} \qquad (16)$$

$$R_{13}C_{11}+R_{23}C_{12}-(R_{E3}+R_{31}+R_{32})C_{13}=-R_{s13} \qquad (17)$$

where

R_{s11}, R_{s12}, R_{s13} = rate of source type 1 in zone 1, etc., nL/h,

and the other terms are similar to those defined on p. 20. Note: These equations assume that steady state applies (i.e., the pollutant rate is constant) and that there are no reactive losses. Radcn would be an example of a pollutant meeting these assumptions; NO_2 from a combustion source would require the addition of a first-order decay term ($k_{11}V_1C_{11}$) to the right-hand term of each equation and quite possibly time-dependent solution.

Since all the rates of exfiltration, R_E, and rates of air exchange, e.g., R_{12}, were determined from the tracer measurements (see Appendix), Eqs. 15 to 17 can be used in two ways: 1) if the pollutant concentrations in the 3 zones are measured, the source rates can be computed, and 2) if the source rates are known or assumed, the concentrations in the 3 zones can be solved from the 3 simultaneous equations. The latter will be demonstrated to examine the variability in zone concentrations with source location, to demonstrate the best procedure for determining the total infiltration rates in multizone homes using a single, constant emission rate tracer source such as SF_6 [24], popular because of the simplicity of the sampling and analysis equipment, and to indicate the information that is not available with simplified approaches.

Consider a 3-zone house (e.g., 2nd floor, 1st floor, basement) in which a simple, single tracer approach is to be used. An overall material balance gives

$$R_{E1}C_{11} + R_{E2}C_{12} + R_{E3}C_{13} = R_{s1} \qquad (18)$$

Eq. 18 can be solved for the total exfiltration rate, R_{ET}, which is the sum of the individual exfiltration rates, if those rates are equal (a situation which will be shown not to be the case) or if the concentrations in each zone are equal (i.e., $C_{11}=C_{12}=C_{13}= \bar{C}$). Then Eq. 18 becomes

$$R_{ET}\,\bar{C} = R_{s1} \qquad (19)$$

i.e., a single tracer is applicable. Because this approach is popular, the question to be addressed here is under what circumstances are the concentrations in each zone of a 2-story house with a basement equal and, if not, what are the extents of the errors. Replacing each of the concentration terms in Eqs. 15 to 17 with $\overline{C}$ gives

$$R_{I1}\overline{C} = R_{s11} \tag{20}$$

$$R_{I2}\overline{C} = R_{s12} \tag{21}$$

$$R_{I3}\overline{C} = R_{s13} \tag{22}$$

Thus Eqs. 20-22 show that in a multizoned structure, to attain a uniform tracer concentration within the entire building requires a source strength in each zone in proportion to the infiltration rate in each zone, which is the principal of the automated constant concentration approach [25]. Manual deployment of properly sized sources in each zone would, of course, require prior knowledge of the individual zone infiltration rates to achieve constant concentration in the entire building; the magnitude of errors associated with determining the total infiltration rate using equal source strengths will be demonstrated for three previously discussed Long Island homes. But first, a consideration of attics and crawl spaces will be made.

<u>The potential effect of an attic and crawl space</u> on the indoor air quality (IAQ) within the living zone are demonstrated for the energy efficient test house belonging to the University of Illinois, a one-story ranch home. The flow results, shown schematically in Fig. 13, were calculated from the PFT concentration data shown in Table 21. That the attic, main floor living zone, and crawl space are 3 separate zones is clear

from the different concentrations of each PFT found in each zone; note also that the tracer concentration was the highest in the zone in which it was deployed, a necessary but not sufficient condition for all flow rates to be computed as positive values. The standard deviation of the living zone concentrations for PFT 2, which was deployed in that zone, was quite high, indicating that uniform tagging of that zone was not achieved.

Fig. 13 shows that there is almost as much air exchange between the living zone and the attic, contrary to I'Anson's results [11], as there is between the living zone and the outside air, indicating that the attic considered as a zone can help to distinguish leaks in the ceiling from those in the walls such as door and window penetrations, important in weatherization studies.

Table 22 shows the expected concentrations in the 3 zones for a 1000 nL/h source located alternatively in each zone. When located in the crawl space (case 1), the concentration in the living zone (4.39 nL/m^3) is 35% of the value when the source is in the living zone (12.41 nL/m^3). With the source in the attic, the proportion is only 3.2% (0.40 divided by 12.41 nL/m^3). Since attics do not generally contain any significant pollutant sources and, further, since they are usually well ventilated, for example, nearly 3.0 ACH in this case, which is typical [11], there is no need to consider attics in usual IAQ studies.

On the other hand, crawl spaces can be a significant source of soil gas containing radon [15]. If radon concentrations in the living and crawl zones were measured in the proportion of 4.39 to 9.27, then the entire source of radon would have been located in the crawl space; if the ratio were higher, then Eqs. 15-17 could be used to find the source strength in both zones. A positive source in the living zone usually can be traced to radon in the domestic water supply. Further, as shown in Fig. 13, the crawl space contributed a greater flow of air into the living zone than did the outside walls which is important to know for weatherization programs.

Infiltration ACH and effective ACH values are given in Table 21. The first is an indicator of the amount of fresh air entering each zone directly from outside; it is simply the infiltration rate divided by the zone volume. The second ACH, labeled the effective ACH, is an indicator of the total fresh air coming from outside and effectively coming from the other zones; it is simply the rate of a source in that zone divided by the concentration in that zone and the volume of the zone, that is, the apparent single zone infiltration rate. For example, the source rate in the living zone of the Illinois house (2906 nL/h, Table 21) divided by the concentration (36.07 nL/m^3) gives an effective infiltration rate of 80.57 m^3/h which, divided by the zone volume (507 m^3), gives the effective ACH (0.159 h^{-1}) shown in the table.

The effective or single zone infiltration rate can be used to compute effective source strengths from measured concentrations. From the 12.41 nL/m^3 value in Table 22 (case 2), multiplying by the effective infiltration rate of 80.57 m^3/h gives the effective source rate of 1000 nL/h. However, for case 1, using the 4.39 nL/m^3 concentration, the effective source rate in the living zone is computed to be 353.7 nL/h, which is equivalent to the actual crawl space source rate of 1000 nL/h times the portion of crawl space air entering the living zone (40.8 m^3/h) relative to the total air leaving the crawl space (116.3 m^3/h), i.e.,

$$1000 \times \frac{R_{32}}{(R_{32} + R_{31} + R_{E3})}$$

Thus, the effective or single-zone ACH can be used to determine an effective pollutant source strength, but it cannot be used to quantify the actual source strength if it is located in another zone. This can only be done with the multiple tracers approach using the material balance equations such as Eqs. 15-17 for a 3-zone case.

The three Long Island houses had an unheated basement and two floors that were heated. The Goodrich house, built in 1952, was a New England cape cod style that had substantial additions to the first floor. The Dietz house, built in 1972, was a colonial model, also one of a number in a development. The unoccupied Brookhaven (BNL) House, completed in September 1980, for energy conservation research, was specially equipped to reduce air infiltration. For each house, the basement was isolated from the first floor by a door which was closed at all times; the first and second floors were connected by an open staircase. Oil-fired hot water convective heating was used in the Goodrich and Dietz houses, supplemented by an airtight wood-burning stove in each first floor; forced hot air was provided to the first floor of the Brookhaven House with vents in the ceiling to provide natural draft to the second floor where the return air grill was located.

Table 21 gives the measured test results for a February 1984 winter period, which were representative of the entire heating season results, and Fig. 14 shows the schematic of the flow patterns in the 3 houses. For the Dietz and Brookhaven houses, the concentrations were highest in the zones in which the source was deployed. The test failed in the Goodrich house; for the source deployed on the first floor, its concentration was higher on the second floor (17.0) compared to the first floor (15.6 nL/m^3). This was determined to be due to one of the first floor sources being placed on an inside wall in the living room near the staircase to the upstairs; apparently the air flow to upstairs carried most of the tracer from that source up the stairs instead of mixing within the room. As indicated earlier in the instructions, it is important to place the sources near outside walls. The result of this error was the calculation of a significantly large negative infiltration rate (-18.5 m^3/h in Table 21) on the second floor (note that the flow information in the table is slightly different than in the figure because of a correction made after the drawing was completed). Modifying the Goodrich concentrations slightly by reversing the concentrations of PFT 2 on the first and second floor gave the new results shown in Table 21. All the flow terms were now positive as anticipated; note that the total air changes per hour (ACH) remained essentially the same as did most of the other flow rates. Further details on the flow pattern differences between the three houses are given elsewhere [26].

The concentrations expected in each zone of the three homes for a 1000 nL/h source alternatively located in each of the zones are shown as cases 2-4 in Table 23. The concentration differences are interesting; for case 2, the concentration is much higher on the second floor in the Dietz house compared to the others because it had little infiltration and exfiltration from that zone. Also note the low concentrations in the basement for the Dietz and Goodrich homes because of the little flow into the basement from either the second or first floors; in contrast, the BNL house had a modest basement concentration from a source on the second floor because of significant flows from the first and second floors into the basement (cf. Fig. 14).

CO from an unvented gas or kerosene space heater represents an example of a steady-state source on the first floor. For this case 3, the relationship between second and first floor concentrations is about the same in all three homes, that is, slightly lower on the second floor compared to the first floor, despite the large differences in flow patterns. It would appear to be a general conclusion that for a source deployed on the first floor of any two-story house and, for that matter, for a source deployed in the basement (case 4), the concentration on the second floor will be about 91 ± 4% of the value on the first floor. Thus, someone sleeping in a bedroom on the second floor will be exposed to a not-much-lower level than on the first floor. Of course, the modeling assumption here is that the first floor is a well-mixed zone such that the concentration is everywhere the same, including the first floor room containing the pollutant source. In many homes, the open nature of the first floor will lend towards good mixing; in others, a somewhat isolated room with the source might properly be treated as a separate zone from the balance of the first floor. In any event, the concentrations upstairs for nonreactive pollutants will not be significantly less than in the balance of the first floor.

Radon from soil gas penetration into basements is a form of steady-state source exemplified by case 4 in Table 23. For all three homes built on the same soil and assuming the same source strength term (e.g., 1000 nCi/h), the radon concentration would be much higher in the Dietz basement (21.9 nCi/m^3 or 21.9 pCi/L), by about a factor of 3 to 5, compared to the other two basement values for case 4 (8.5 and 4.8 pCi/L). The same ratio holds for the living zone radon concentrations.

A closer comparison of the Dietz and BNL houses with respect to the supposed basement radon source is revealing. Assuming both had the same source rate of 1000 nCi/h and having measured the whole house infiltration rates as 0.195 and 0.288 h^{-1}, respectively (shown as case 1 in Table 23), one would expect whole house concentrations (case 6) of 8.2 and 5.3 pCi/L, respectively, for the Dietz and BNL houses, a ratio of about 1.5 to 1. Instead, the "measured" concentrations (case 4) of 8.3 and 3.1 pCi/L, respectively, were in a proportion of 2.7 to 1, a significant difference. This is a good example of living zone radon concentrations correlating poorly with whole house, i.e., single zone, infiltration rates. Even the ratio of the average radon concentrations in the whole house ($\overline{C}_{21B}$), 12.71/4.94 or 2.6 to 1, indicated poor correlation with the whole house ACHs.

The reason can be seen in the basement flow patterns as revealed by the 3-zone BNL/AIMS results (cf. Fig. 14). For the Dietz house, the portion of basement air entering the living zone is 100% because there is no exfiltrating air (R_{E3} = $-0.8\ m^3/h$). However, in the BNL house the portion is

$$\frac{40.7 + 16.4}{40.7 + 16.4 + 74.2} = 0.43$$

or only 43%. Thus, the BNL house radon source term is effectively much less. This cannot be explained with anything less than basement-living zone 2-zone tracer measurements.

Built on the same soil with the same basement structure exposed to the soil, the BNL/AIMS flow patterns reveal a potential for further exacerbation of the potential radon problem in the Dietz house compared to the others. The zero exfiltration rate from the Dietz basement implies the existence of a significant sub-atmospheric pressure in the basement, which, of course, can mean a larger driving force for soil gas penetration than in a basement with a high exfiltration rate such as in the other two houses. This can be further seen by the very large basement to first floor stack effect (cf. Fig. 14), i.e., the flow up (46.6) divided by the flow down (0.7 m^3/h) or 67 to 1; for the BNL basement, the stack effect is only 1.6 to 1, and for the Goodrich basement, 21 to 1. It is expected that such multizone measurements will significantly extend our understanding of this important IAQ concern.

How to perform single-zone measurements in multizone houses is also revealed in Table 23. Although, as discussed above, such measurements miss a lot of important information, many researchers prefer the single-zone approach because they have only one tracer source, usually SF_6. A first and simple approach is to uniformly divide the source strength between each floor (case 5), remembering that the true infiltration rate can only be obtained when the concentration in each zone is equal (case 6). Indeed, for equal source rates in each zone (case 5), there was a significant difference in the concentration in each zone and in that distribution for the three houses. Comparing the average whole house concentration ($\overline{C}_{21B}$) for case 5 with the true average (case 6), shows that for the Dietz house, the result is 2.9% high; for the BNL house, 0.9% low; and for the Goodrich house, 4.1% low.

The actual source rate distribution required to attain equal zone concentrations are shown in case 6. The results show that the distribution should be for the second floor, 4 to 11%; for the 1st floor, 37 to 56%, and for the basement, 37 to 59%. Obviously, a good compromise would be 50% on the first floor and 50% in the basement with no source on the second floor; the errors with this general approach would probably always be less than 1 to 2% in houses with natural convection. Further studies are needed in forced convection homes.

Single-zone measurements of the living zone of a 2-story house is also demonstrated in Table 23. Case 7 assumes equal source strengths of the second and first floors and case 8 gives the source strength distribution for equal concentrations on the two floors. This is an important approach for researchers that have two tracers and want to tag the basement with one and the living zone of a 2-story house with the other. For a 50-50 distribution on the second and first floors (case 7), the error in the living zone average concentration ($\bar{C}_{21}$) compared to the true value (case 8) is 14.9% high for the Dietz house; 3.2% low for the BNL house; and 9.8% low for the Goodrich house.

The actual source rate distribution required to attain equal concentrations on the first and second floors are shown in case 8. Thus, the distribution is weighted heavily towards the first floor, even in houses with forced air convection such as the BNL house (76%), compared to natural convection (92 to 94%). Placing the living zone source entirely on the first floor (case 3) gives errors of -2.1%, 2.9%, and 1.7%, respectively, for the three houses, and the requirement of a uniform concentration in the first and second floor for a source in the basement (case 4), which is required for correct solution of this 2-zone approach, is seen to be nicely approximated. Thus, this approach will give a correct picture of the interaction between a basement and the living zone; of course, it cannot give the correct second floor concentration for a source on that floor.

The choice of PFT source types with zone location is important in multizone structures. Because of the stack effect in all houses, a source placed on the second floor will have a very low concentration in the basement (case 2 in Table 23). To improve the precision of its measurement in the basement, the second floor tracer selected should be one with the highest emission rate (cf. Table 1) and the highest detectability, i.e., the earliest eluting tracer on the gas chromatograph (GC) column (Fig. 7). Thus the choice for the second floor tracer in a 3-zone study is either PDCB or PMCP. The same reasoning extended to the other floors dictated that PMCH be used on the first floor and PDCH in the basement. The use of PDCB in one zone and PMCP in another zone in a 3-zone building should be avoided because those two tracers elute very close to each other (Fig. 7) and are therefore difficult to quantify without using special GC conditions.

In stacked 4-zone structures, when both PDCB and PMCP must be used, the correct choice for the uppermost zone is PDCB, followed by PMCP in the next lower zone. When two components elute next to each other, a small quantity of the first eluting component next to a large amount of the second component is always easier to detect than the reverse situation. Placing PDCB in the highest zone guarantees the proper peak size order in each zone except the uppermost zone; but in that zone the PMCP concentration will also be high because of the stack effect.

A significant diurnal effect on ACH exists in houses because of the large swing in outside temperatures between day and night. With passive sampler measurements over a period of a few days to weeks, this effect is not discernable but is adequately integrated to obtain an average infiltration rate [19]. Two programmable samplers collecting 4-h integrated samples for almost 4 days in the BNL house, one sampling upstairs (second floor) and the other downstairs (first floor), gave the computed infiltration rates shown in Fig. 15. The diurnal trend is clearly evident, with maxima and minima occurring at about 0300 and 1500 hours, respectively. Such detailed measurements may be important in more comprehensive studies on IAQ and energy flow calculations.

CONCLUSIONS

From the detailed studies on the PFT sources, for which four types currently exist, it was shown that they can be manufactured with a very reproducible (±2%) and constant emission rate, essentially constant for the lifetime of the sources (2 to 7 years). By using silicone rubber plugs cut from extruded rubber cord, the reproducibility has been improved to within less than ±0.5%. The current temperature sensitivity of the source rate, about 15%/3°C, is sometimes a problem in field studies. Further studies with other rubber materials may reduce that dependence; preliminary tests with buna rubber show about one-half that dependence, but the emission rates are 20-fold lower.

The passive samplers (CATS) were simple to manufacture and very reproducible in their sampling rates, within ±2%.

Although the gas chromatograph analysis system for the passive samplers is complex, each step in the automated sequence is important. With temperature programming of the main column, multiple CATS can be analyzed for 4 PFTs on a 13-min cycle; new techniques are being explored to both improve the GC separation of the PFTs and to shorten the analysis time, primarily by separating the precut column from the main column and providing individually optimized temperature programming. Further work should also be done on improving the linearity of the electron capture detector in order to simplify the calibration procedures.

The field deployment of PFT soures in homes for the purposes of establishing a uniform tracer concentration on each floor required generally two sources per floor. Detailed studies in two-story houses showed that the concentrations were quite uniform (±3%) on the first floor, which is usually more open in structure than the compartmentalized nature of the second floor containing bedrooms, where variability was usually within ±10 to 15% when bedroom doors were always open but sometimes as poor as ±50% when bedroom doors were periodically closed. By placing sources near the outside walls, usually one at each extreme end of a floor, the flow dynamics provided good mixing. But the door to any room containing a source or being sampled must remain open. In multiple floor homes, the highest emission rate source type is preferred on the uppermost floor (i.e., PDCB) and the lowest rate source in the basement (i.e., PDCH). In cases where some bedroom doors are periodically closed, suspending the source in the hall, abut 40-cm from the ceiling and near the bedroom doors, may be preferable; tests are being conducted.

Sampling was generally done by placing the samplers near an inside wall. This allowed good mixing of the emitted PFT vapors with the room air before encountering the sampler. The exact siting of sources and samplers should consider the internal flow dynamics of the house. Warm air within a meter of the ceiling usually flows toward the outside walls where it is cooled, sinks, and returns inwardly toward the center of the floor (e.g., to the hall). On the second floor, some of this returning air will flow down the staircase and pour out within a meter or so of the floor on the first floor. Flowing up the staircase will be a portion of the air on the first floor within a meter or so of the ceiling. Quite obviously, placing a source, meant to tag the first floor, near a staircase leading upstairs, might lead to short-circuiting of some of the tracer to the second floor. Such locations must be avoided.

The BNL/AIMS technique has been satisfactorily validated against SF_6 decay and constant source rate methods in homes and recently in a laboratory chamber versus CO_2 decay measurements [19]. The reproducibility of the system in identical homes located even in different cities was within ±7%.

Multizone measurements in a ranch house with an attic and a crawl space showed that considering the attic as a zone was unnecessary for IAQ studies. It was shown, however, that a significant portion of the living zone air can be exchanged with the attic, an important consideration in weatherization studies. Crawl spaces were shown to be important in both weatherization and IAQ studies because a significant portion of air entering the first floor of a house comes from the crawl space. This can have important implications on energy balances [23] and on IAQ studies, since such zones are the source of indoor radon.

Detailed studes in three two-story homes with basements showed both some extreme differences and similarities. In all three, for a source on the first floor, the concentration on the second floor was generally about 90% of that on the first floor. This provided the interesting observation that to tag the first and second floors to simulate a single, well-mixed zone, a source need only be distributed in the first floor. All three showed extreme differences in the interaction between the basement and the first floor and in the exfiltration patterns from the basements and the second floors, each of which would cause demonstrated differences in the expected indoor air quality for given pollutant source rates and locations.

A generalized weather correlation was successfully developed in which each house was characterized by a specific leakage factor, L, which was the whole house ACH normalized to a fixed function dependent only on inside-outside temperature difference, the wind speed to the 1.5 power, and a terrain factor. For ten homes, L varied from 1.3 to 2.3, and for one home built in 1952, its value was 4.5. With a subjective estimate of the terrain factor, a single measurement period would provide an indication of L; two or more measurements would give an independent measure of the terrain factor as well. Field tests of the applicability of this ACH weather correlation in quantifying reduction in air infiltration due to weatherization efforts are currently under way.

ACKNOWLEDGMENT

To the researchers who performed many of the field experiments in homes and provided the meteorological data, appreciation is expressed. A special thanks is extended to G. Senum and T. D'Ottavio for contributing valuable suggestions and input along the stages of this study. Support from the U.S. Department of Energy Offices of Building Energy Research and Development and of Health and Environmental Research is gratefully acknowledged.

REFERENCES

[1] Spengler, J.D. and Sexton, K., "Indoor air pollution: a public health perspective," Science, Vol. 221, No. 4605, July 1983, pp. 9-17.

[2] Dietz, R.N. and Cote, E.A., "Air infiltration measurements in a home using a convenient perfluorocarbon tracer technique," Environment International, Vol. 8, No. 1-6, 1982, pp. 419-433.

[3] Kronvall, J., "Tracer gas techniques for ventilation measurements: a 1981 state of the art review," in Studies in Building Physics, A.-S. Anderson, Ed., Report TVBH-3007, Lund Institute of Technology, Lund, Sweden, 1981, pp. 81-94.

[4] Sherman, M.H. and Grimsrud, D.T., "Infiltration-pressurization correlation: simplified physical modeling," LBL-10163, Lawrence Berkeley Laboratory, Berkeley, Calif., 1980.

[5] Dietz, R.N., Goodrich, R.W., Cote, E.A., and Wieser, R.F., "Brookhaven air infiltration measurement system (BNL/AIMS) description and applications," BNL-33846, Brookhaven National Laboratory, Upton, N.Y., August 1983.

[6] Ferber, G.J., Telegadas, K., Heffter, J.L., Dickson, C.R., Dietz, R.N., and Krey, P.W., "Demonstration of a long-range atmospheric tracer system using perfluorocarbons," ERL ARL-101, NOAA Air Resources Laboratories, Rockville, Md., April 1981.

[7] Dietz, R.N. and Dabberdt, W.F., "Gaseous tracer technology and applications," BNL-33585, Brookhaven National Laboratory, Upton, N.Y., July 1983.

[8] Senum, G.I., Gergley, R.P., Ferreri, E.M., Greene, M.W., and Dietz, R.N., "Final report of the evaluation of vapor taggants and substrates for the tagging of blasting caps," BNL-51232, Brookhaven National Laboratory, Upton, N.Y., March 1980.

[9] Hunt, C.M., King, J.C., and Trechsel, H.R., Eds., "Building air change rate and infiltration measurements," ASTM STP 719, American Society for Testing and Materials, Pa., 1980.

[10] Hernandez, T.L. and Ring, J.W., "Indoor radon source fluxes: experimental tests of a two-chamber model," Environment International, Vol. 8, No. 1-6, 1982, pp. 45-57.

[11] I'Anson, S.J., Irwin, C., and Howarth, A.T., "Air flow measurement using three tracer gases," Building and Environment, Vol. 17, No. 4, 1982, pp. 245-252.

[12] Perera, M.D.A.E.S., "Review of techniques for measuring ventilation rates in multi-celled buildings," in Proceedings of the EC Contractors' Meeting on Natural Ventilation, Brussels, September 30, 1982, Building Research Establishment, Garston, England, 1982.

[13] Maldonado, E.A.B., "A method to characterize air exchange in residences for evaluation of indoor air quality," Ph.D. dissertation, Iowa State University, Ames, Iowa, 1982.

[14] Ruckdeschel, R.F., "Basic scientific subroutines Vol. 1," Byte/McGraw-Hill, Peterborough, N.H., 1981.

[15] Bruno, R.C., "Sources of indoor radon in houses: a review," Air Pollution Control Association Journal, Vol. 33, No. 2, 1983, pp. 105-109.

[16] Judekis, H.S. and Wren, A.G., "Laboratory measurements of NO and NO_2 depositions onto soil and cement surfaces," Atmospheric Environment, Vol. 12, 1978, pp. 2315-2319.

[17] Lovelock, J.E., "The electron capture detector theory and practice," Journal of Chromatography, Vol. 99, 1974, pp. 3-12.

[18] Quackenboss, J. Personal communication (1983).

[19] Leaderer, B.P., Schaap, L., and Dietz, R.N., "Evaluation of the perfluorocarbon tracer technique for determining infiltration rates in residences," February 1985, submitted for publication in Environmental Science and Technology.

[20] Wang, Sr., F.S. and Sepsy, C.F., "Field studies of air tightness of residential buildings," in Ref. 9, pp. 24-35.

[21] Malik, S., "Field studies of dependence of air infiltration on outside temperature and wind," Energy and Buildings, Vol. 1, No. 3, 1978, pp. 281-292.

[22] Dietz, R.N., Goodrich, R.W., Cote, E.A., and Wieser, R.F., "Application of perfluorocarbon tracers to multizone air flow measurements in mechanically and naturally ventilated buildings," Presented at the ASHRAE seminar on Tracer Gas Measurements of Ventilation Rates in Mechanically Ventilated Buildings, Chicago, January 30, 1985, BNL 35249, Brookhaven National Laboratory, Upton, N.Y., August 1984.

[23] D'Ottavio, T.W. and Dietz, R.N., "Errors resulting from the use of single zone ventilation models on multi-zone buildings: implications for energy conservation and indoor air quality studies," to be presented at the ASHRAE Symposium on Multi-Cell Infiltration, Honolulu, June 1985, Brookhaven National Laboratory, Upton, N.Y., February 1985.

[24] Tolzke, D., Quackenboss, J., Kaarakka, P., and Flukenger, J. "A modified tracer gas infiltration method for use in a residential indoor air quality/weatherization study," in Indoor Air, Vol. 5, B. Berglund, T. Lindvall, and J. Sandell, Eds., Swedish Council for Building Research, Stockholm, 1984, pp. 459-464.

[25] Sinden, F.W., Multi-chamber theory of air infiltration, Building and Environment, Vol. 13, 1982, pp. 21-28.

[26] Dietz, R.N., D'Ottavio, T.W., and Goodrich, R.W., "Seasonal effects on multi-zone air infiltration in some typical U.S. homes using a passive perfluorocarbon tracer technique," to be presented at the Copenhagen '85 World Congress on Heating, Ventilating, and Air Conditioning, Copenhagen, August 25-30, 1985, BNL 36151, Brookhaven National Laboratory, Upton, N.Y., February 1985.

Table 1
PFT Source Rates and Lifetimes

T[a]	Vapor Pressure at 25°C, atm	Background Ambient Conc., fL/L[b]	Liquid Density, g/mL	Molecular Weight	Permeation Rate at 25°C, nL/min	Lifetime,[c] years
CH	0.046	25.6	1.85	400	12 to 20	7.2 to 4.3
CH	0.14	3.6	1.79	350	24 to 35	4.0 to 2.7
CP	0.44	2.8	1.70	300	40 to 55	2.6 to 1.9
CB	0.50	0.35	1.67	300	36 to 50	2.9 to 2.1

a)
DCH (perfluorodimethylcyclohexane), PMCH (the methylcyclohexane), and PMCP (the ethylcyclopentane) are available from Manchem, Inc., Princeton, N.J., PDCB (the imethylcyclobutane) is available from PCR Research Chemicals, Gainesville, FL.

b)
oncentration units: fL/L represents femtoliters per liter (i.e., parts-per-quadrillion or 10^{-15}); L/L represents picoliters/liters (i.e., parts-per-trillion or 10^{-12}).

c)
ased on an initial liquid PFT content of 0.4 mL.

$$\Delta t = \frac{V}{\dot{V}} = \frac{0{,}4\ mL}{\frac{12\ mL}{min}} = \frac{0{,}4 \cdot 10^{-3}\ \ell\ min}{12 \cdot 10^{-9}\ \ell} = 33333\ min = 555\ h = 23\ Tage$$

Table 2

GC Specification and Conditions

All columns (including catalyst beds and adsorbent trap) are made with 3.2-mm (0.125-in.) OD stainless steel tubing

Main column	: 1.2-m (4-ft) long packed with 0.1% SP-1000 on Carbopack C (Supelco, Inc., Bellefonte, Pa.)
Precut columns	: 1.2-m (4-ft) long Porasil F followed by 0.3-m (1-ft) long of 0.1% SP-1000 on Carbopack C
Column oven	: 140°C
Precut catalyst	: 10.1-cm (4-in.) long packed with Pd (1%) on polyethylenimine/SiO_2- Royer Pd catalyst (Strem Chemicals, Inc., Newburyport, Mass.); 200°C
Main catalyst	: 3.2-cm (1.25-in.) long packed similarly; 200°C
Carrier gas	: 5% H_2 in N_2 at 25 and 20 mL/min, respectively, through the precut and main columns
Porapack QS trap	: 10.1-cm (4-in.) long packed with Porapak QS
Permeation dryer	: 1.2-m (4-ft) long Nafion dryer (Permapure Products Inc., Oceanport, N.J., Model MD-125-48S) located in the top of GC (~35°C)
ECD	: 180°C

Table 3

Gas chromatograph[a] sequence of events

Event Time, min	Event Code	Event	Event Status
0.00		System steps to next sample tube; starts event clock	
0.01	.01	Recorder starts	Off
0.01	.14	QS/Sampler heating relay switches to QS trap	On
0.02	.10	Desorption power turned on	On
0.02	.12	High power position	On
0.35	.13	Low power position	Off
0.50	.08	Sample in QS trap injected (i.e., V_4 on)	On
1.60	.09	V_4 off	Off
1.60	.11	Desorption power turned off	Off
1.62	.15	QS/Sampler relay switches to sampler	Off
2.30	.06	V_3 on	On
4.95	.04	V_2 on	On
5.00	.02	V_1 on	On
5.00	.10	Desorption power turned on	On
5.00	.12	High power position	On
5.40	.13	Low power position (not used for BATS tubes)	Off
5.70	.08	V_4 on	On
7.30	.11	Desorption power turned off	Off
7.60	.09	V_4 off	Off
7.70	.07	V_3 off	Off
7.75	.03	V_1 off	Off
7.80	.05	V_2 off	Off
8.01	.00	Recorder off	On

[a] External events designation and codes:

		Valves				Heating		
Item:	Recorder	Sample(V_1)	Precut(V_2)	Flow Dir.(V_3)	QS(V_4)	Desorp. Power	High Low	QS Sampler
Event On	.00	.02	.04	.06	.08	.10	.12	.14
Event Off	.01	.03	.05	.07	.09	.11	.13	.15

Table 4
Effect of changing concentrations on calculated average exfiltration rate. Assume R_s is 1500 nL/h

	Case 1		Case 2	
Period	C, nL/m^3	R_E, m^3/h	C, nL/m^3	R_E m^3/h
1	17	88.2	25	60
2	16	93.8	20	75
3	15	100.0	15	100
4	14	107.1	10	150
5	13	115.4	5	300
Avg.	15 ± 1.6	100.9 ± 10.7	15 ± 7.9	137.0 ± 97.3
R_E,calc.[a]		100.0 ± 10.5		100.0 ± 52.7
Diff.[b]		0.9 ± 15.0		37.0 ± 110.7

[a] Calculated from Eq. 3

[b] Difference between the true average R_E and that calculated by Eq. 3.

Table 5
Stability of PFT source rates with time; determined gravimetrically at 25°C

PFT Type	Code[a]	Permeation Rate and Std. Dev., nL/min Nov. 82 - Jan. 83[c]	 May 83 - Sept. 83[d]	Ratio: $\frac{1983}{1982}$
PDCH	3-1-S40	19.43 ± 0.29	20.27 ± 0.11	1.043 ± 0.022
	2	19.83 ± 0.09	19.81 ± 0.10	0.999 ± 0.010
	3	16.22 ± 0.19*	16.82 ± 0.08*	1.037 ± 0.017
	4	19.62 ± 0.08	19.84 ± 0.09	1.011 ± 0.009
	5	19.40 ± 0.32	20.30 ± 0.20	1.046 ± 0.028
	6	19.01 ± 0.27	19.85 ± 0.12	1.044 ± 0.021
	Avg.[b]	19.46 ± 0.30	20.01 ± 0.25	1.030 ± 0.020
PMCH	2-1-S40	33.74 ± 0.16	33.55 ± 0.11	0.994 ± 0.008
	2	36.12 ± 0.21	35.92 ± 0.12	0.994 ± 0.009
	3	33.62 ± 0.16	33.35 ± 0.12	0.992 ± 0.008
	4	33.09 ± 0.16	32.92 ± 0.12	0.995 ± 0.008
	5	37.72 ± 0.21*	37.04 ± 0.06*	0.982 ± 0.007
	6	34.57 ± 0.16	34.35 ± 0.14	0.994 ± 0.009
	Avg.[b]	34.23 ± 1.18	34.02 ± 1.18	0.992 ± 0.005
PDCB	1-1-S40	49.34 ± 0.18	48.98 ± 0.24	0.993 ± 0.009
	2	49.80 ± 0.21	49.66 ± 0.29	0.997 ± 0.010
	3	52.10 ± 0.18	51.74 ± 0.22	0.993 ± 0.008
	4	50.30 ± 0.24	49.98 ± 0.14	0.994 ± 0.008
	5	48.09 ± 0.21	47.96 ± 0.17	0.997 ± 0.008
	6	48.88 ± 0.21	48.53 ± 0.15	0.993 ± 0.007
	Avg.	49.75 ± 1.38	49.48 ± 1.33	0.995 ± 0.002

[a] 3-1-S40 means tracer 3 (i.e., PDCH), source No. 1, silicone rubber plug of 40 hardness.

[b] Asterisked values excluded from average.

[c] Perkin-Elmer Electrobalance

High precision analytical balance

Table 6

Stability of PFT source rates with time; determined gravimetrically at 25°C

PFT		Permeation Rate and Std. Dev., nL/min		1983
Type	Code[a]	Nov. 82 - Jan 83[c]	May 83 - Sept. 83[d]	Ratio: 1982
PDCH	3-1-S70	12.54 ± 0.05	12.69 ± 0.07	1.012 ± 0.010
	2	12.47 ± 0.08	12.61 ± 0.08	1.011 ± 0.013
	3	12.54 ± 0.07	12.66 ± 0.19	1.010 ± 0.021
	4	12.64 ± 0.08	12.80 ± 0.08	1.013 ± 0.013
	5	12.35 ± 0.09	12.55 ± 0.07	1.016 ± 0.013
	6	12.61 ± 0.08	12.84 ± 0.08	1.018 ± 0.013
	Avg.	12.53 ± 0.10	12.69 ± 0.11	1.013 ± 0.003
PMCH	2-1-S70	25.75 ± 0.12	25.55 ± 0.25	0.992 ± 0.014
	2	24.19 ± 0.13	23.98 ± 0.11	0.991 ± 0.010
	3	24.84 ± 0.12	24.66 ± 0.12	0.993 ± 0.010
	4	30.26 ± 0.15*	29.90 ± 0.10*	0.988 ± 0.008
	5	24.14 ± 0.12	23.94 ± 0.12	0.992 ± 0.010
	6	23.70 ± 0.13	23.54 ± 0.12	0.993 ± 0.010
	Avg.[b]	24.52 ± 0.80	24.33 ± 0.79	0.992 ± 0.002
PDCB	1-1-S70	35.10 ± 0.13	35.35 ± 0.28	1.007 ± 0.012
	2	35.50 ± 0.04	35.71 ± 0.25	1.006 ± 0.008
	3	36.55 ± 0.03	36.75 ± 0.27	1.005 ± 0.008
	4	36.21 ± 0.06	36.30 ± 0.18	1.002 ± 0.007
	5	35.64 ± 0.05	--	--
	6	37.53 ± 0.05	37.63 ± 0.18	1.003 ± 0.006
	Avg.	36.09 ± 0.88	36.35 ± 0.90	1.005 ± 0.002

[a-d] Same as Table 5.

Table 7
PFT Source Calibration; Gravimetric versus Chromatographic

Source Type	Source Code	Emission Rate at 25°, nL/min		
		Gravimetric	Chromatographic	Grav./Chrom.
PDCB	1-1-S70	35.4 ± 0.3	38.8	0.91
PMCH	2-1-S40	33.6 ± 0.1	31.1 ± 1.0	1.08 ± 0.04
PMCH	2-7-S60	35.7 ± 0.1	32.9 ± 1.2	1.09 ± 0.04
PDCB	1-1-S70	35.4 ± 0.3	38.1 ± 2.8	0.93 ± 0.07
"	1-2-S70	35.7 ± 0.3	38.4 ± 2.9	0.93 ± 0.07
"	1-1-S40	49.0 ± 0.2	49.7 ± 3.9	0.99 ± 0.08
"	1-2-S40	49.7 ± 0.3	50.3 ± 3.7	0.99 ± 0.07
"	1-7-S60	53.3 ± 0.1	55.1 ± 4.1	0.97 ± 0.07
PDCH	3-1-S70	12.7 ± 0.1	13.3 ± 2.8	0.95 ± 0.17
"	3-2-S70	12.6 ± 0.1	13.2 ± 2.5	0.95 ± 0.16
"	3-3-S70	12.7 ± 0.2	13.7 ± 2.7	0.93 ± 0.16
"	3-1-S80	12.8 ± 0.1	12.6 ± 2.5	1.02 ± 0.17
			Avg.=	0.98 ± 0.06

Table 8
PFT Source Activation Energy

Source Type	Source Code	Activation Energy, kcal/mole	Gravimetric Emission Rate, nL/mi	
			at 25°C	at 37°C
Immediate (<1 h) Temperature Effect[a]				
PDCH	3-2-S60	4.00 ± 0.14	20.1 ± 0.2	
"	3-4-S40	4.99 ± 0.15	19.8 ± 0.1	
"	3-1-S70	5.16 ± 0.13	12.7 ± 0.1	
"	3-2-S70	5.33 ± 0.24	12.6 ± 0.1	
"	3-3-S70	4.59 ± 0.11	12.7 ± 0.2	
"	3-9-S70	6.53 ± 0.24	11.9[a]	
"	3-1-S80	6.94 ± 0.20	12.8 ± 0.1	
PDCB	1-7-S60	1.70 ± 0.02	53.3 ± 0.1	
"	1-1-S40	3.06 ± 0.05	49.0 ± 0.2	
"	1-2-S40	3.26 ± 0.05	49.7 ± 0.3	
"	1-1-S70	3.86 ± 0.04	35.4 ± 0.3	
"	1-2-S70	3.66 ± 0.03	35.7 ± 0.3	
Long-Term (>1 week) Temperature Effect[b]				
PDCH	TC-185	8.6 ± 1.5	16.6 ± 0.6	29.1 ± 0.
"	3-3-S70	8.7 ± 0.4	12.7 ± 0.2	22.4 ± 0.
PMCH	2-_-S80[c]	7.9 ± 1.3	29.9 ± 1.1	43.4 ± 0.
PDCB	1-7-S60	6.2 ± 0.1	53.3 ± 0.1	79.8 ± 0.
"	1-_-S80[c]	8.0 ± 1.2	38.8 ± 0.4	65.3 ± 1.
Avg. Long-Term ΔH		7.9 ± 1.0		

[a] Estimated from chromatographic measurements between 25° and 37°C.
[b] Placed in oven to obtain gravimetric rate at 37°C for comparison with rate at 25°C
[c] Represents average from three sources.

Table 9
Passive Sampler (CATS) Leakage Rate with Caps On

Type of cap	Rate of leakage, %
Vinyl (yellow)	~0.5
Auster (black)	0.6 to 0.8
Girard U103B	0.060
Girard U103B-PU	<0.0004

[a] Leakage rate as percentage of sampling rate.

Table 10
Effect of Temperature on CATS

CATS No.	Temp. °C	Tracer response, arbitrary units			
		PMCH		PDCH	
		Meas.	Expected	Meas.	Expected
334	25	124.4		170.4	
335	"	122.6		169.4	
336	"	116.8		159.7	
340	"	127.4		174.5	
342	"	123.4		171.1	
		123±4	123	169±5	169
331	35	126.0		177.0	
332	"	126.4		172.0	
333	"	123.0		167.5	
		125±2	125	172±5	172
337	50	137.2		188.8	
338	"	136.8		183.6	
339	"	135.2		187.1	
		136±1	128	186±3	176

Table 11
Reproducibility of Multiple CATS Sampling
(Sampling for 45.3 h)

CATS analysis No.	Tracer concentration, pL/L			Tracer concentration ratios		
	PDCB	PMCH	PDCH	PDCB/PMCH	PDCH/PMCH	PDCB/PDCH
1	3.407	37.29	35.12	0.09134	0.9416	0.09701
2	3.518	38.34	36.17	0.09176	0.9435	0.09725
3	3.403	38.53	35.34	0.08831*	0.9170*	0.09630
4	3.503	39.04	36.60	0.08974	0.9377	0.09571
5	3.444	37.73	36.26	0.09128	0.9610	0.09498
6	3.612	39.54	36.51	0.09134	0.9234*	0.09892*
7	3.523	38.41	36.17	0.09170	0.9416	0.09738
8	3.629	39.27	37.18	0.09242	0.9469	0.09760
9	3.524	38.76	36.78	0.09093	0.9488	0.09583
10	3.541	38.85	36.80	0.09115	0.9472	0.09624
11	3.596	39.17	37.27	0.09179	0.9515	0.09647
12	3.502	38.19	35.97	0.09168	0.9419	0.09734
13	3.584	38.79	36.96	0.09242	0.9530	0.09697
14	3.591	38.79	37.11	0.09256	0.9566	0.09676
15	3.654	40.07	38.03	0.09117	0.9489	0.09609
16	3.592	39.04	37.92	0.09200	0.9714	0.09471
17	3.527	38.71	37.56	0.09111	0.9703	0.09390
18	3.577	38.64	36.74	0.09258	0.9508	0.09738
19	3.468	37.57	36.03	0.09231	0.9589	0.09626
20	3.413	38.38	36.81	0.08893*	0.9592	0.09271*
avg.	3.530	38.66	36.67	0.09133	0.9486	0.09629
std. dev.	±0.075	±0.66	±0.76	±0.00115	±0.0133	±0.00141
rel. std. dev.	(±2.1%)	(±1.7%)	(±2.1%)	(±1.26%)	(±1.41%)	(±1.46%)
avg.[a]				0.09163	0.9517	0.09634
std. dev.				±0.00072	±0.0096	±0.00102
rel. std. dev.				(±0.78%)	(±1.01%)	(±1.06%)

[a] Values of 2 points with asterisks excluded.

Table 12
PFT Analyses of Six Background Air Samples

Sample Volume, L	PFT Ambient Concentrations, fL/L[a]			
	PDCB	PMCP	PMCH	PDCH
24.94	0.373	2.76	3.72	26.8
24.36	0.340	2.76	3.57	27.4
24.88	0.359	2.68	3.53	24.9
24.11	0.329	2.69	3.47	23.6
23.37	0.290	2.59	3.50	25.5
22.11	0.383	2.79	3.70	25.5
Avg.	0.346	2.71	3.58	25.6
	± 0.034	± 0.07	± 0.10	± 1.4

[a] fL/L is equivalent to 0.001 pL/L.

Table 13
PFT Concentration Distribution within the BNL House[a]
(1/19/83 to 1/21/83)

CATS Sampler No.	Location	Floor	Comments	PFT[b] Concentration, pL/L	
				PMCH	PDCH
577	L.R. coffee table	1st	Next to No. 581	9.37	7.62
581	"	"		9.42	7.40
574	L.R. TV	"	Far from PDCH	9.12	7.85
585	Dining area	"	Next to PDCH source	9.65	7.93
573	L.R. fireplace	"		9.56	7.53
575	Mas. bedroom	2nd	Near door to hall	17.0	7.37
576	"	"	Nearer PMCH source	22.0	7.07
584	Bedroom 2	"	Door closed; no source	10.4	8.34
583	Bedroom 1	"	On dresser in sun	19.2	7.43
580	"	"	On dresser in shade	18.8	7.78

[a] House consists of basement and 1st and 2nd floors.

[b] PFT sources were as follows:

Floor vol., m^3	PFT Source		PFT Location	Avg. PFT conc., pL/L	
	Type	Rate, nL/h		PMCH	PDCH
240	PDCH	2035	Dining area and fam. rm.	9.42 ± 0.18	7.67 ± 0.20
215	PMCH	3749	Mas. bedroom and bedrm. 1	19.2 ± 1.8	7.41 ± 0.25

Table 14
PFT Concentration Distribution within the BNL House
(9/16/83 to 9/30/83)

CATS Sampler No.	Location	Floor	Comments	PFT[a] Concentration, pL/L		
				PMCH	PDCH	PDC
925	Mas. bedrm.	2nd	PMCH source in room	52.9	17.8	5.7
816	Bedroom 2	"	"	53.6	17.9	5.4
944	Bathroom	"	No source	47.9	17.1	5.4
Avg.				51.5±3.1	17.6±0.4	5.57±0
954	L.R. coffee table	1st	PDCH source in room	16.4	21.9	6.4
838	Kitchen range	"	No source	17.2	21.6	6.8
935	Fam. rm. counter	"	PDCH source in room	18.9	20.7	6.
Avg.				17.5±1.3	21.4±0.6	6.51±0
927	Bsmt. near stairs	Bsmt.	PDCB source in center of room	7.22	4.44	32.3
963	Bsmt. near furnace	"		6.99	4.47	38.7
Avg.				7.11±0.16	4.46±0.02	35.5±

[a] PFT sources were distributed as follows:

Zone	Floor	Floor Vol., m^3	PFT Source		Location
			Type	Rate, nL/h	
1	2nd	215	PMCH	3941	Mas. bedrm. and bedrm. 2
2	1st	240	PDCH	2115	Din. area and fam. rm.
3	Bsmt.	204	PDCB	2004	Center of basement

Table 15
Multiple SF_6 Tracer Decays versus BNL/AIMS[a]
(1700 6/10/82 to 1300 6/30/82)
Chicago Test Home[b]

SF_6 Measurements (LBL)

- 306 measurements at 90 min each (459 of 476-hour period)
- Mean SF_6 air infiltration rate = $0.33\ h^{-1}$

PFT Measurement

- 2 PDCH sources and 4 passive samplers
- Measured PDCH concentrations were as follows:

CATS No.	Location	Floor	PDCH Source	Conc., pL/L
258	Liv. rm.	1st	1	12.0
250	Bedrm.	"	-	8.7
262	Bsmt.	Bsmt.	1	11.1
256	"	"	-	11.3
Avg.			1632 nL/h	10.8 ± 1.2

- Mean PFT infiltration rate = $0.31 \pm 0.04\ h^{-1}$

---

[a] Field measurements conducted by Lawrence Berkeley Laboratory (LBL).
[b] Single-story house with an unfinished basement (481 m^3 total).

Table 16
Comparison of BNL/AIMS with SF_6 Tracer and Blower Door Tests[a]

Method	No. of Homes	Avg. ACH,[b] h^{-1}	Method vs. BNL/AIMS Slope	Method vs. BNL/AIMS Intercept
BNL/AIMS	9	0.39 ± 0.22		
Constant SF_6 rate	8	0.37 ± 0.21	0.82 ± 0.16	0.04
Blower door	9	1.36 ± 0.45	1.01 ± 0.69	0.96

[a] Field tests conducted by the University of Wisconsin.
[b] ACH represents air changes per hour.

Table 17
Tracer Concentrations and Air Infiltration Rates in 5 Swedish Homes

		PDCH Concentration, pL/L				
		1st Floor		2nd Floor		
House Code[a]	Sampling Period	Foyer	Living Rm	Bedrm	Hall	Air Changes, h^{-1}
M4	4/7-5/11/83	27.3	23.6	19.7	20.1	0.70 (± 16%)
M7	4/7-5/11/83	32.9	21.6	25.2	22.1	0.63 (± 21%)
S7	4/1-5/10/83	32.4	22.9	26.4	21.5	0.65 (± 19%)
S8	4/2-5/10/83	32.2	24.5	22.6	25.1	0.59 (± 16%)
S9	4/2-5/10/83	13.2	14.1	6.1	12.4	1.34 (± 32%)
Average:[b]		31.2	23.2	23.5	22.2	0.64 (± 7%)
		(± 8%)	(± 5%)	(± 13%)	(± 9%)	

---

[a] M represents city of Malmö and S, Stockholm.
[b] House S9 excluded from averages.

Table 18
Modeled Infiltration Rates for the NAHB-CCH[a]
Effect of Temperature Difference and Wind Speed

Measurement Period	Avg. Temp. Diff., °C	Avg. Wind Speed, m/s	Average Air Changes per Hour, h^{-1}			
			Meas.	Calc.[b]	Calc.[c]	Diff.,[d] %
Sept. 1982	-	-	0.10	-	-	-
Oct. 1982	7.5	1.61	0.12	0.12	0.13	+7
Nov. 1982	11.5	2.06	0.18	0.18	0.19	+7
Dec. 1982	14.9	1.74	0.21	0.21	0.21	0
Jan. 1983	18.9	1.03	0.22	0.22	0.22	0
Feb. 1983	18.1	0.85	0.20	0.20	0.20	+2
March 1983	12.7	0.89	0.21	0.15	0.15	-28
April 1983	9.4	2.46	0.24	0.18	0.19	-19
May 1983	7.2	1.16	0.37	0.10	0.11	-72
Averages	16.2[e] ±2.9	1.1[e] ±0.4	0.18[f] ±0.05			± 9%[f]

[a] National Association of Home Builders - Conventional Comparison House.

[b] Calculated ACH,h^{-1} = $-(0.01\pm0.01) + (0.0108\pm0.0005)\Delta t + (0.0236\pm0.0024)u^{1.5}$

[c] Calculated ACH, h^{-1} = $L(0.006\ \Delta t + \frac{0.03}{c}u^{1.5})$

where $L = 1.70\pm0.08$ (±4.7%) and $c = 2.3\pm0.23$ (slightly shielded terrain).

[d] Difference is between the second calculated and the measured values.

[e] Average temperature and wind speed was from December to March.

[f] May values excluded from averages.

Table 19

Modeled Infiltration Rates for 7 Canadian Homes versus Temperature Difference and Windspeed

House Code	L	c	2/15-2/28/83			2/28-3/15/83			3/15-3/30/83			4/19-4/29/83			4/29-5/17/83		
			Meas	Calc[a]	Diff,%	Meas	Calc	Diff,%	Meas	Calc	Diff,%	Meas	Calc	Diff,%	Meas	Calc	Diff,%
08	1.93 ± 0.12	7 ± 3	0.28	0.29	+3	0.26	0.28	+6	0.34	0.34	0	0.24	0.23	- 3	0.24	0.17	-31
10	1.47 ± 0.03	21 ± 12	0.19	0.20	+3	0.17	0.17	0	0.21	0.21	0	0.17	0.14	-17	0.16	0.10	-40
20	2.27 ± 0.28	3 ± 1	0.41	0.41	+1	0.40	0.45	+12	0.56	0.55	-2	0.25	0.38	+54	0.19	0.29	+54
28	1.27 ± 0.02	16 ± 6	0.17	0.17	+2	0.15	0.15	+2	0.19	0.19	-1	0.30	0.13	-58	-	0.09	-
32	2.00 ± 0.33	8 ± 13	0.29	0.29	+1	0.24	0.28	+15	0.38	0.34	-11	0.39	0.23	-41	-	0.16	-
34	1.53 ± 0.03	19 ± 10	0.20	0.21	+3	0.18	0.18	0	0.22	0.22	+1	-	0.15	-	0.19	0.10	-47
39	2.28 ± 0.17	18 ± 16	0.29	0.31	+6	0.27	0.27	0	0.30	0.33	+11	0.24	0.22	-7	0.27	0.15	-43
Avg. $\lvert\text{Diff}\rvert$%:					± 3			± 5			± 4			± 30			± 43
Avg. Temp. Diff., °C					20.9			17.0			21.1			13.9			9.1
Avg. Wind Speeds, m/s					3.2			4.5			5.1			4.2			3.8

[a] Calc. $\text{ACH}, h^{-1} = L\,(0.006\ \Delta t + \frac{0.03}{c}\,u^{1.5})$

Table 20
Air Changes Per Hour in Three Long Island Homes versus Temperature Difference and Wind Speed

Approximate Measurement Period[a]	Approx.[b] Temp. Diff., °C	Approx.[b] Wind Speed, m/s	Average Air Changes per Hour (ACH), h^{-1}								
			Dietz House			Brookhaven House			Goodrich House		
			Meas.	Calc.[c]	Diff. %	Meas.	Calc.[c]	Diff. %	Meas.[e]	Calc.[c]	Diff. %
Oct. 1983 (1)	7.2	1.7	-	-	-	0.13	0.13	1	-	-	-
(2)	11.2	1.9	0.17	0.16	-6	0.17	0.19	13	-	-	-
Nov. (1)	11.7	1.7	0.13	0.15	14	0.16	0.19	20	0.53	0.41	-22
(2)	10.2	2.6	0.18	0.17	-6	0.20	0.21	2	0.59	0.47	-20
Dec. (1)	12.7	2.6	0.17	0.20	15	0.21	0.23	12	0.64	0.57	-12
(2)	20	2.4	0.23	0.25	11	-	-	-	0.74	0.74	0
Jan. 1984 (1)	18	2.0	0.23	0.22	-4	-	-	-	0.72	0.69	-5
(2)	21	1.6	0.23	0.23	-2	-	-	-	0.70	0.70	0
Feb. (1)	16	2.2	0.20	0.19	-4	0.29	0.25	-13	0.54	0.60	11
(2)	15	2.7	0.22	0.24	9	0.28	0.25	-13	0.53	0.57	8
March (1)	18.0	2.8	0.29	0.27	-8	0.30	0.30	-2	0.63	0.72	14
(2)	13.7	2.4	0.21	0.20	-5	0.27	0.22	-16	0.62	0.56	-10
April (1)	11.0	2.8	0.21	0.21	-1	0.20	0.22	9	-	-	-
(2)	8.4	2.4	0.19	0.15	-21	0.16	0.16	5	-	-	-
Averages	18.0[d]	2.3[d]	0.21		±9%	0.22		±12%	0.62		±12%
	±2.3	±0.4	±0.04			±0.06			±0.08		

[a] Numbers in parentheses represent 1st and 2nd half of the month

[b] The approximate temperature differences and wind speeds were generally within ±1°C and ±0.1 m/s, respectively, of the actual measurements for each house; exact values were used in the calculation.

[c] Calculated ACH, $h^{-1} = L(0.006\ \Delta t + \frac{0.03}{c}\ u^{1.5})$

House	L	c
Dietz	1.58 ± 0.18 (±12%)	2.5 ± 0.8
Brookhaven	1.68 ± 0.34 (±20%)	1.9 ± 0.6
Goodrich	4.47 ± 0.60 (±14%)	3.0 ± 1.6

[d] Average temperature and wind speed was from mid-December to mid-March.

[e] Living zone (1st and 2nd floor) ACH was used because of non-representative condition in the 3-zone measurements.

Table 21

BNL/AIMS Results for Several 3-Zone House Tests. Measured PFT Concentrations

House	Zone	Vol., m^3	Source Rate, nL/h	Average Tracer Concentrations,[a] nL/m^3			Exfil. Rate, m^3/h	Infiltration		Eff.[c] ACH, h^{-1}	Exchange Rates,[d] m^3/h, from Zone - to Zone -		
				PFT 1	PFT 2	PFT 3		Rate, m^3/h	ACH,[b] h^{-1}		1	2	3
Illinois	1. Attic	212	1578	2.45 ± 2.06	1.72 ± 1.15	0.92 ± 0.49	627.0	614.0	2.90	3.04	-	29.7	8.7
(3/14-	2. Liv.	507	2906	0.62 ± 0.11	36.07 ± 8.85	13.11 ± 0.17	40.5	28.6	0.06	0.16	18.2	-	40.8
4/11/84)	3. Crawl	179	2989	0.25 ± 0.06	5.50 ± 1.16	27.70 ± 2.00	66.8	91.7	0.51	0.60	7.3	17.4	-
	Totals	898					734.3	734.3	0.818[e]				
Dietz	1. 2nd	255	1319	19.22 ± 1.50	23.51 ± 0.29	9.08 ± 0.19	19.6	7.2	0.03	0.27	-	116.6	0.1
(2/1-	2. 1st	250	3045	9.12 ± 2.39	24.99 ± 0.39	9.63 ± 0.23	103.5	69.9	0.28	0.49	104.3	-	46.6
2/22/84)	3. Bsmt	123	1153	0.17 ± 0.02	0.44 ± 0.06	25.30 ± 4.29	-0.8	45.1	0.37	0.37	0.1	0.7	-
	Totals	628					122.3	122.2	0.195[e]				
BNL	1. 2nd	215	3208	26.64 ± 2.18	10.76 ± 0.21	4.34 ± 0.19	89.4	21.1	0.10	0.56	-	211.7	16.4
(2/1-	2. 1st	240	1544	15.78 ± 1.96	12.41 ± 0.69	4.21 ± 0.31	26.3	75.5	0.31	0.52	148.1	-	40.7
2/15/84)	3. Bsmt	204	1356	5.54 ± 0.14	3.44 ± 0.08	11.55 ± 0.00	74.2	93.3	0.46	0.58	11.8	26.2	-
	Totals	659					189.9	189.9	0.288[e]				
Goodrich	1. 2nd	122	1743	10.49 ± 5.72	17.03 ± 0.91	2.50 ± 0.06	154.7	-18.5	-0.15	1.36	-	234.5	-1.9
(2/1-	2. 1st	272	3477	2.14 ± 0.70	15.55 ± 1.37	2.34 ± 0.53	51.2	155.8	0.57	0.82	58.4	-	75.0
2/15/84)	3. Bsmt	153	1471	0.08 ± 0.02	0.34 ± 0.08	7.07 ± 2.18	136.4	205.1	1.34	1.36	0.9	3.6	-
	Totals	547					342.3	342.4	0.626[e]				
Goodrich	1. 2nd	122	1743	10.5	15.5	2.5	152.4	14.3	0.12		-	185.1	3.7
(modified)	2. 1st	272	3477	2.1	17.0	2.6	63.0	127.1	0.47		49.7	-	74.5
	3. Bsmt	153	1471	0.08	0.34	7.1	129.9	203.9	1.33		0.9	3.3	-
	Totals	547					345.3	345.3	0.631[e]				

[a] Average concentration for 2 or 3 CATS in each zone. PFT 1 was deployed in zone 1, etc.

[b] The infiltration ACH was the zone infiltration rate, m^3/h, divided by the zone volume, m^3.

[c] The effective ACH was the zone source rate divided by the source concentration in that zone and by the zone volume.

[d] Air exchange rate example for the Illinois house: the rate from zone 1 to zone 2, R_{12}, was 18.2 m^3/h.

[e] The total house ACH was the total infiltration rate divided by the total volume.

Table 22
Expected Zone Concentrations in the Illinois House for a Source in Different Locations

	Source Rate, nL/h, and Location			Calculated[a] Zone Concentrations, nL/m^3		
Case	Attic	Living	Crawl	Attic	Living	Crawl
1	-	-	1000	0.32	4.39	9.27
2	-	1000	-	0.59	12.41	1.89
3	1000	-	-	1.55	0.40	0.16

[a] By normalizing the measured concentrations in Table 21 with the known source strengths or by Eq. 15-17 using the flow rates in Table 21.

Table 23

Evaluations of Multizone Houses as Single-Zone Buildings.
Expected Zone concentrations for One Type of Source in Different Locations

			Source Location and Rate,[a] nL/h			Calculated[b] Zone Concentrations, nL/m^3					Total Infil.		Living Zone Infiltration	
House	Case	Calculation Basis	2nd	1st	Bsmt	2nd	1st	Bsmt	$\bar{C}_{21B}$	$\bar{C}_{21}$	Rate m^3/h	ACH h^{-1}	Rate m^3/h	ACH h^{-1}
Dietz (2/1-22/84)	1	3-Zone results									122.2	0.195		
	2	Source on 2nd flr	1000	-	-	14.6	6.9	0.1	-	10.74	-	-	93.1	0.184
	3	Source on 1st flr	-	1000	-	7.7	8.2	0.1	-	7.96	-	-	125.6	0.249
	4	Source in bsmt	-	-	1000	7.9	8.3	21.9	12.71	8.10	78.7	0.125	123.5	0.244
	5	Equal source rates (3)	333	333	333	10.0	7.8	7.4	8.42	-	118.8	0.189	-	-
	6	Equal zone conc. (3)	60	571	369	8.2	8.2	8.2	8.18	-	122.2	0.195	-	-
	7	Equal source rates (liv)	500	500	-	11.1	7.6	0.1	-	9.34	-	-	107.0	0.212
	8	Equal zone conc. (liv)	60	940	-	8.1	8.1	0.1	-	8.13	-	-	123.0	0.244
BNL (2/1-15/84)	1	3-Zone results									189.9	0.288		
	2	Source on 2nd flr	1000	-	-	8.3	4.9	1.7	-	6.61	-	-	151.2	0.332
	3	Source on 1st flr	-	1000	-	7.0	8.0	2.2	-	7.50	-	-	133.3	0.293
	4	Source in bsmt	-	-	1000	3.2	3.1	8.5	4.94	-	202.3	0.307	-	-
	5	Equal source rates (3)	333	333	333	6.2	5.4	4.2	5.22	-	191.4	0.290	-	-
	6	Equal zone conc. (3)	112	397	491	5.3	5.3	5.3	5.27	-	189.9	0.288	-	-
	7	Equal source rates (liv)	500	500	-	7.6	6.5	2.0	-	7.06	-	-	141.7	0.311
	8	Equal zone conc. (liv)	240	760	-	7.3	7.3	2.1	-	7.29	-	-	137.2	0.301
Goodrich (2/1-15/84)	1	3-Zone results									345.3	0.631		
	2	Source on 2nd flr	1000	-	-	6.0	1.2	0.1	-	3.61	-	-	276.7	0.702
	3	Source on 1st flr	-	1000	-	4.5	4.9	0.1	-	4.67	-	-	214.0	0.543
	4	Source in bsmt	-	-	1000	1.7	1.8	4.8	2.77	-	360.8	0.660	-	-
	5	Equal source rates (3)	333	333	333	4.1	2.6	1.7	2.78	-	359.5	0.657	-	-
	6	Equal zones conc. (3)	41	368	591	2.9	2.9	2.9	2.90	-	345.3	0.631	-	-
	7	Equal source rates (liv)	500	500	-	5.2	3.1	0.1	-	4.14	-	-	241.3	0.612
	8	Equal zone conc. (liv)	82	918	-	4.6	4.6	0.1	-	4.59	-	-	218.0	0.553

---

[a] The source rates for cases 6 and 8 were calculated from Eqs. 15-17 by letting all 3 (case 6) or the 2nd and 1st floor (liv-case 8) zone concentrations be equal and the sum of the source rates be 1000 nL/h.

[b] Calculated from Eqs. 15-17 using the flow rates given in Table 21. $\bar{C}_{21B}$ is the avg. conc. for 3 zones and $\bar{C}_{21}$, for the 2nd and 1st floors (living zone).

FIGURE CAPTIONS

Fig. 1 Diagram of the PFT source configuration.

Fig. 2 Passive sampler with polyurethane rubber caps.

Fig. 3 Passive sampler thermal desorption rack.

Fig. 4 Schematic of laboratory GC analyzer. V_1 is the sample valve; V_2, the precut valve; V_3, the flow direction valve; and V_4, the Porapak QS valve. Each is shown in its "on" position; in its "off" position, the valve slots are rotated 90° counterclockwise.

Fig. 5 Model considered for a two-zone house.

Fig. 6 Time required for new sources to attain a steady emission rate. Two upper curves (□,■) are PDCH sources with 60-durometer silicone rubber plugs (S60); the next (Δ), PMCH (S60); the last (O), PMCH (S80).

Fig. 7 Chromatograms of two 25-L ambient air samples with the GC specifications shown in Table 2. The unknown peak after PDCB is PMCP.

Fig. 8 Response of the ECD-GC to PDCH.

Fig. 9 Histograms of air changes per hour for three separate studies.

Fig. 10 Dependence of air infiltration rate on inside-outside temperature difference.

Fig. 11 Dependence of infiltration rate on wind speed.

Fig. 12 Seasonal trends in infiltration rates for seven Canadian houses.

Fig. 13 Three-zone flow rates determined for a ranch house.

Fig. 14 Three-zone flow rates determined for the periods indicated in the three Long Island houses. All flow rates are in m^3/h; the ACH values are the infiltration rates divided by the zone volumes.

Fig. 15 Diurnal effect on two-zone infiltration rates determined on a 4-h frequency using programmable samplers.

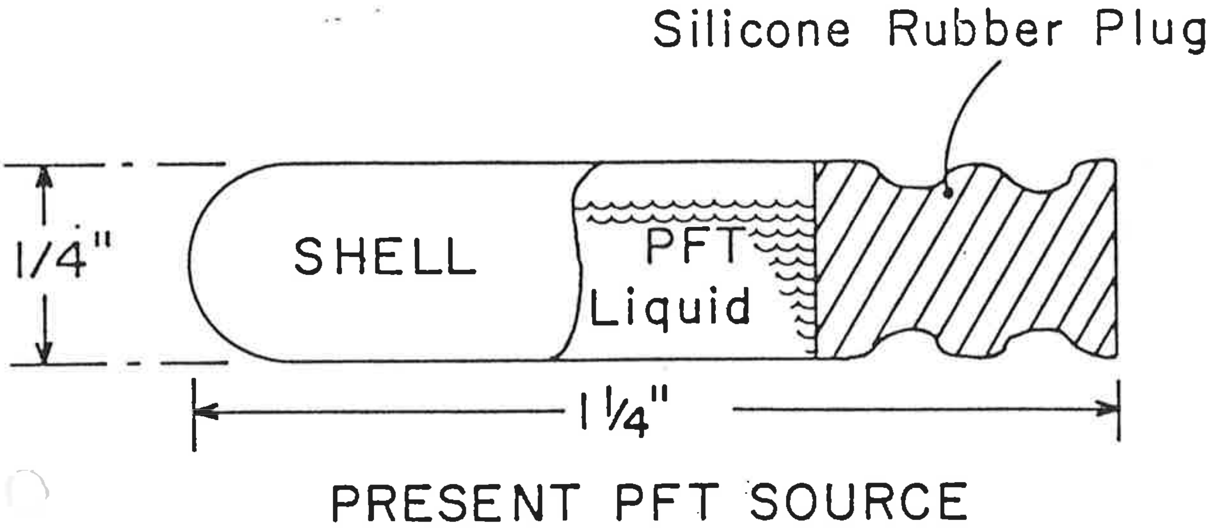
Silicone Rubber Plug
1/4"
SHELL
PFT
Liquid
1 1/4"
PRESENT PFT SOURCE

Fig. 1

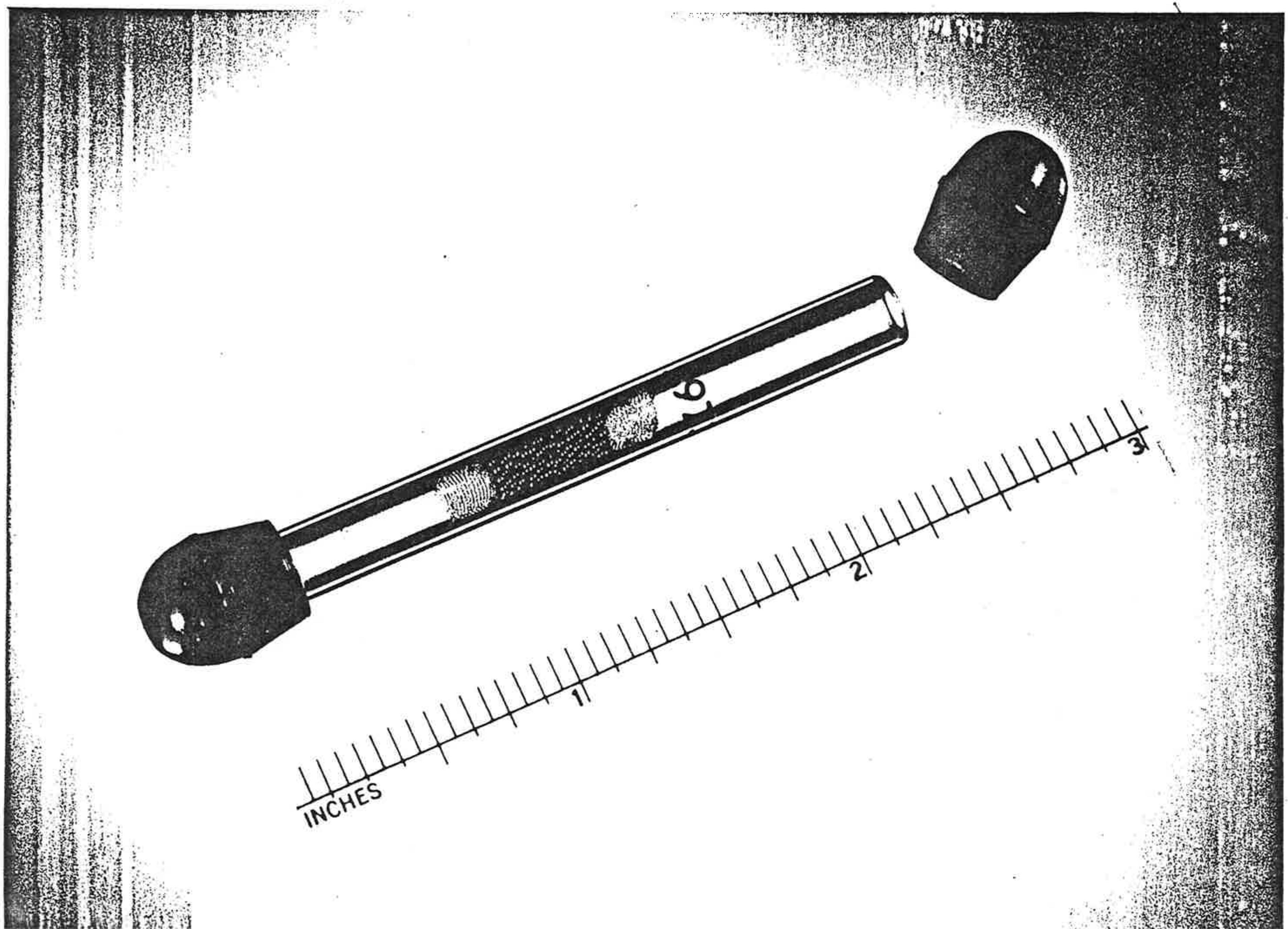
INCHES
1
2
3
16

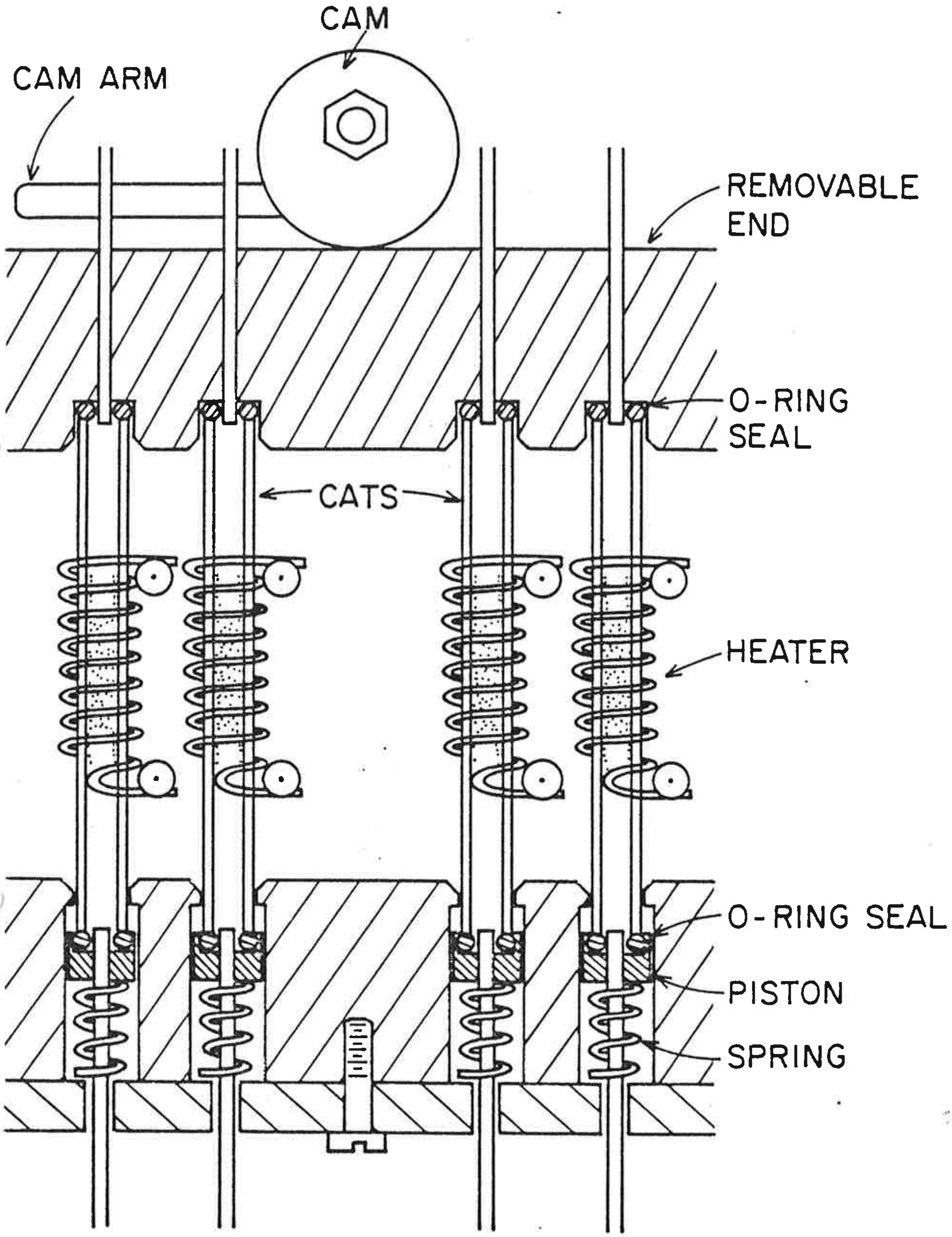

THERMAL DESORPTION APPARATUS

Fig. 3

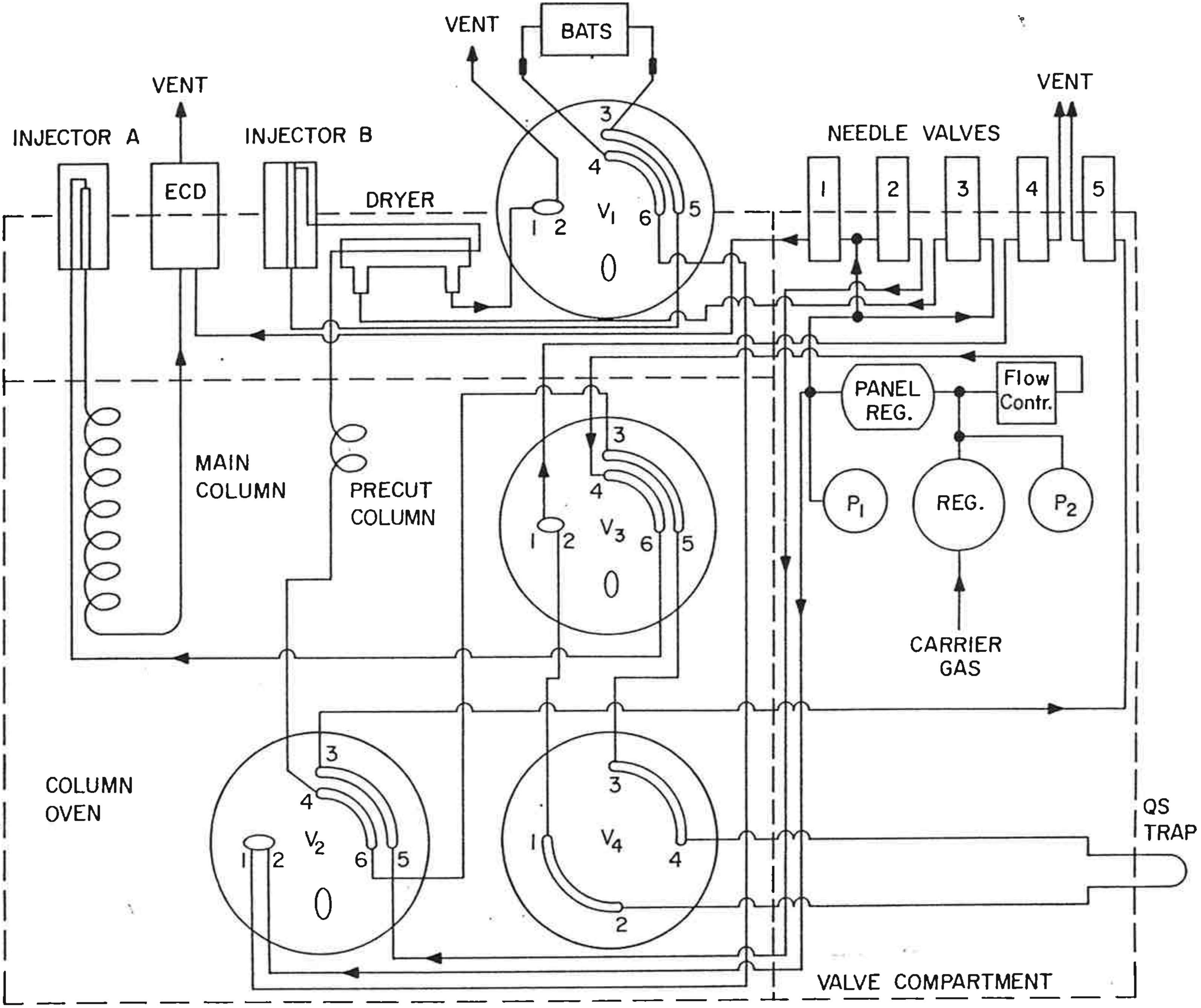
VENT
BATS
VENT
VENT
INJECTOR A
ECD
INJECTOR B
DRYER
NEEDLE VALVES
1
2
3
4
5
V1
1 2 3 4 5 6
0
PANEL REG.
Flow Contr.
P1
REG.
P2
CARRIER GAS
MAIN COLUMN
PRECUT COLUMN
V3
1 2 3 4 5 6
0
COLUMN OVEN
V2
1 2 3 4 5 6
0
V4
1 2 3 4
QS TRAP
VALVE COMPARTMENT

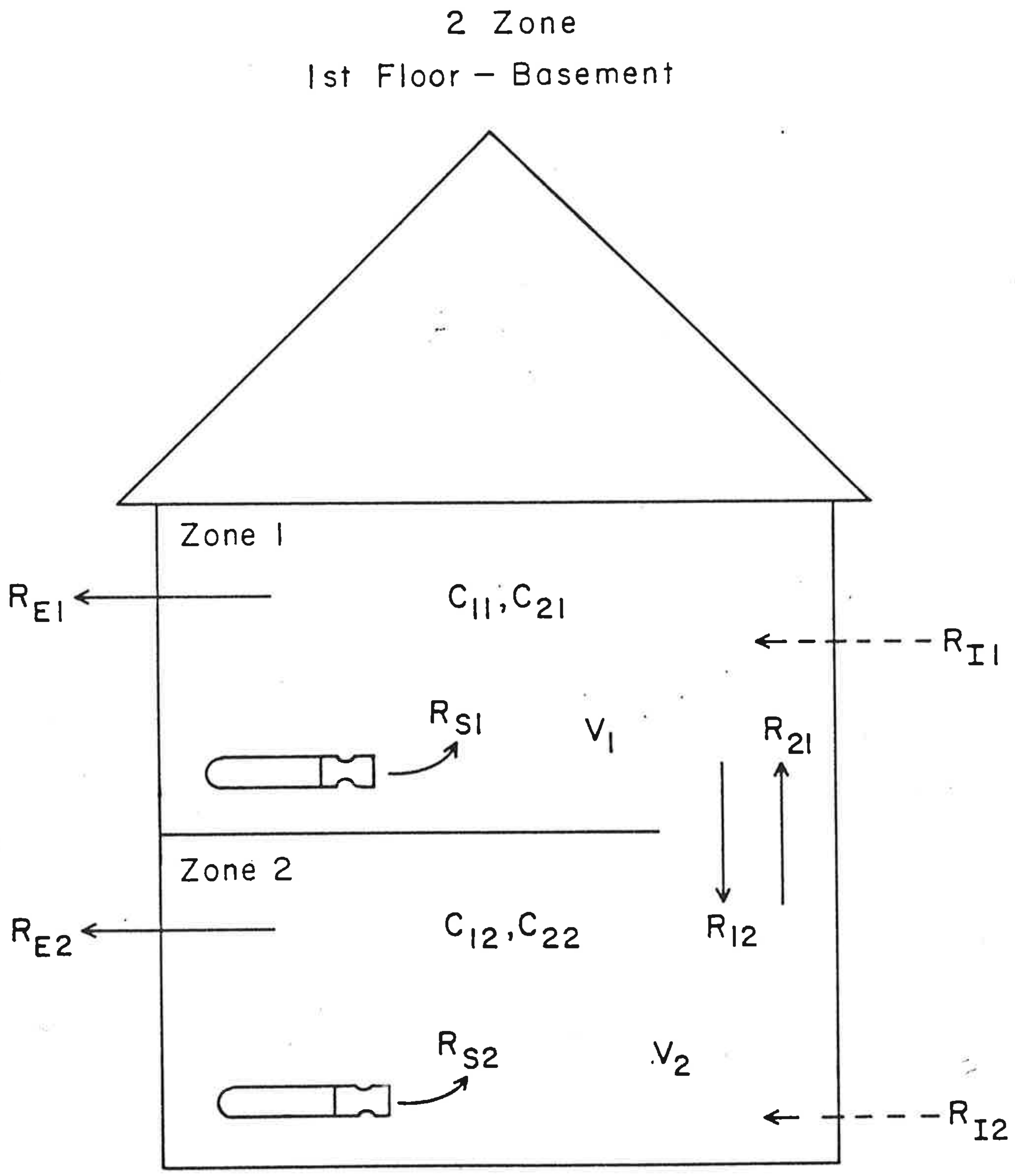
2 Zone
1st Floor – Basement
Zone 1
R_{E1}
C_{11}, C_{21}
R_{I1}
R_{S1}
V_1
R_{21}
Zone 2
R_{E2}
C_{12}, C_{22}
R_{12}
R_{S2}
V_2
R_{I2}

Fig. 5

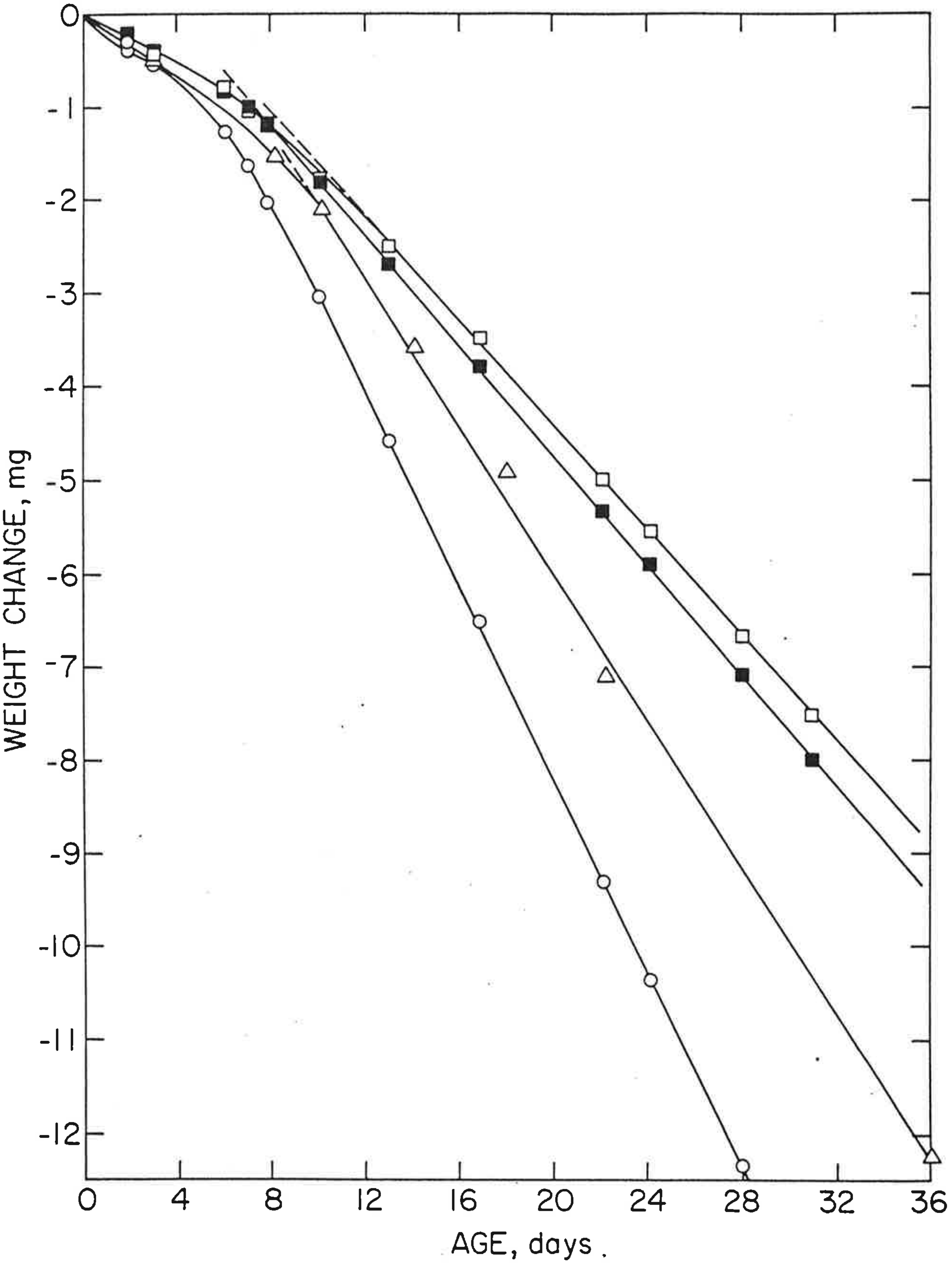
WEIGHT CHANGE, mg
0
-1
-2
-3
-4
-5
-6
-7
-8
-9
-10
-11
-12
AGE, days
0
4
8
12
16
20
24
28
32
36

Fig. 6

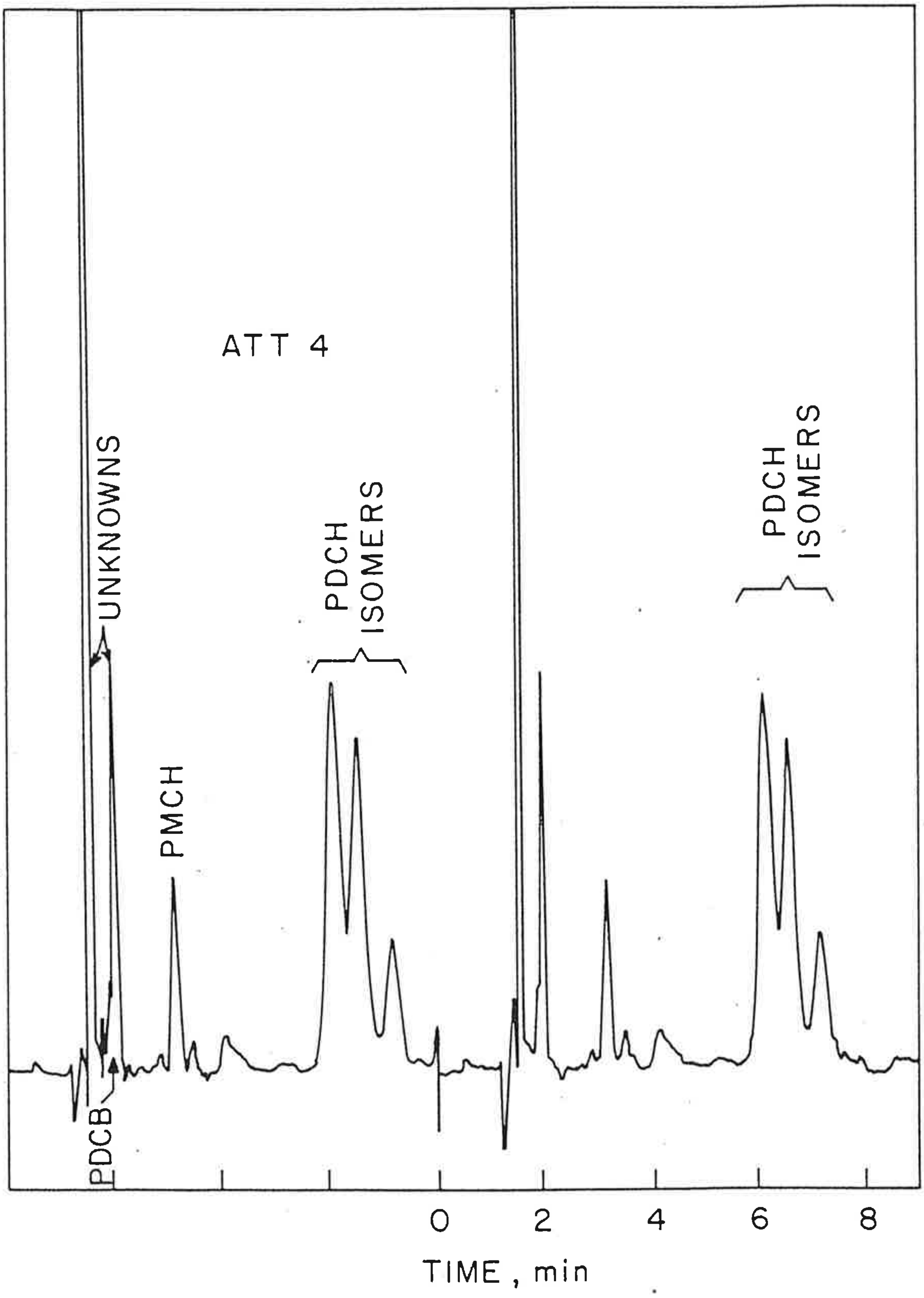
ATT 4
UNKNOWNS
PDCB
PMCH
PDCH ISOMERS
PDCH ISOMERS
0
2
4
6
8
TIME, min

Fig. 7

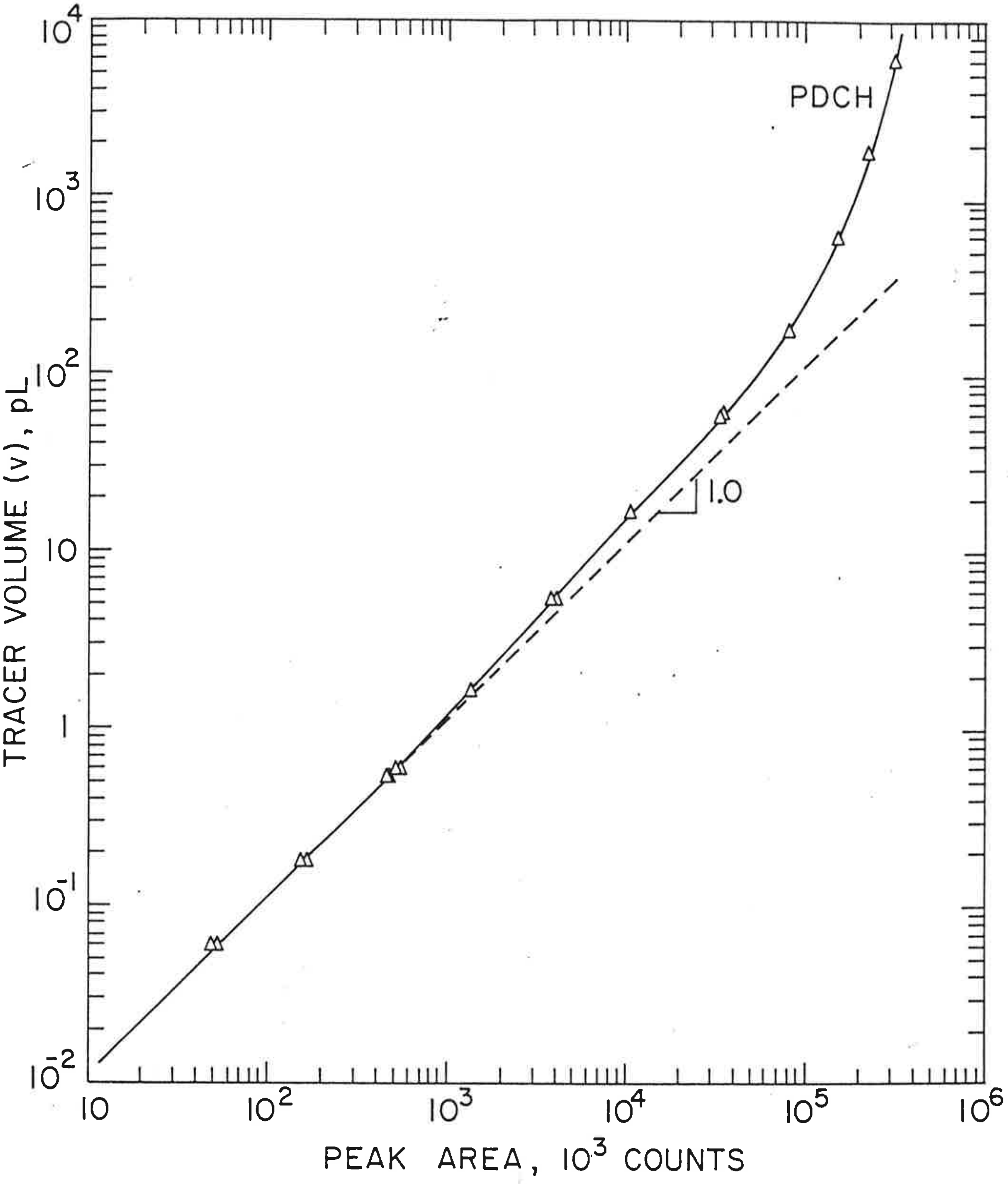
TRACER VOLUME (v), pL
PEAK AREA, 10^3 COUNTS
PDCH
1.0
10^{-2}
10^{-1}
1
10
10^2
10^3
10^4
10
10^2
10^3
10^4
10^5
10^6

Fig. 8

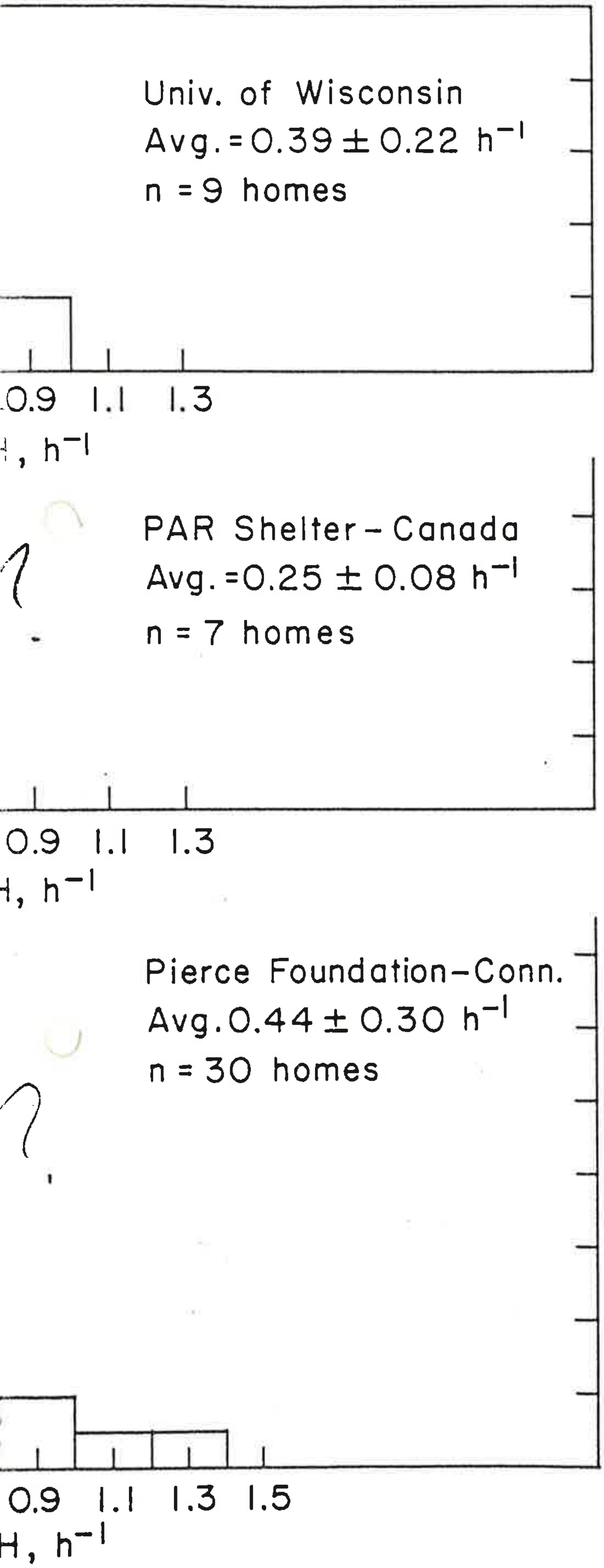

Fig. 9

?

?

?

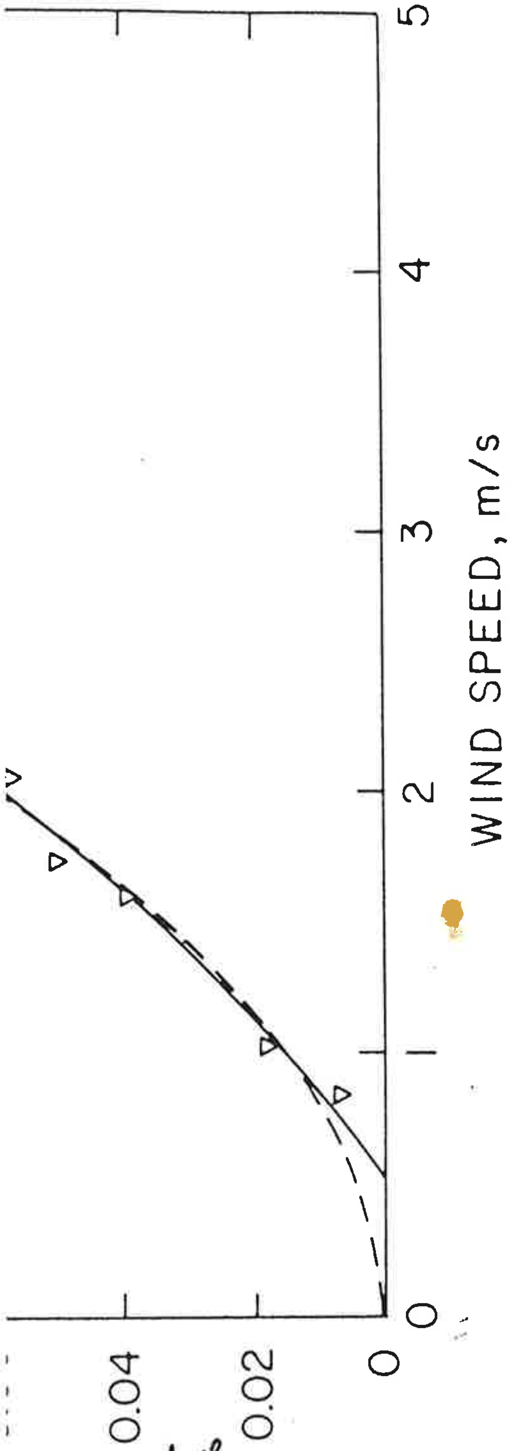

Fig. 11

a poor place to save paper.

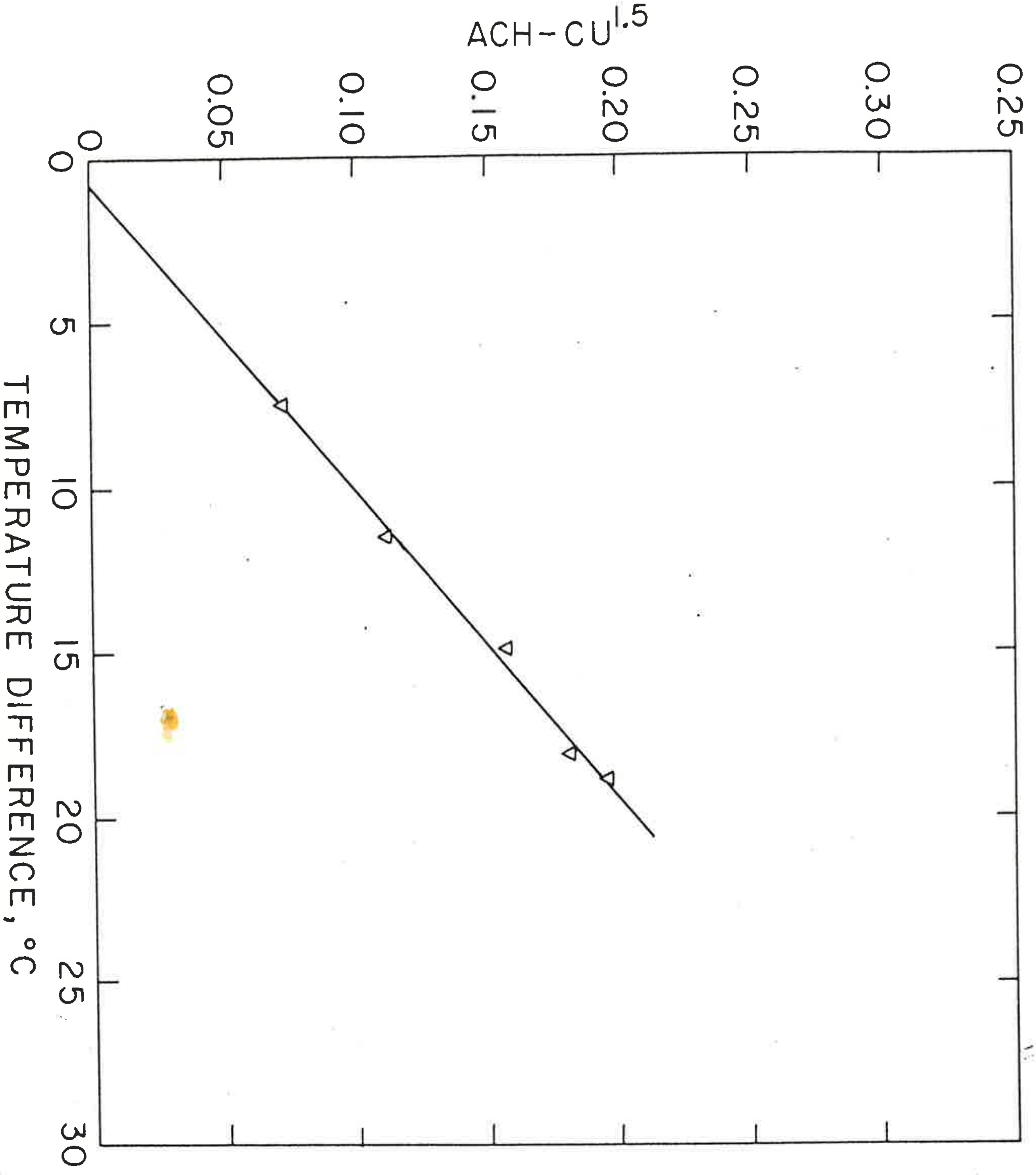
ACH-CU$^{1.5}$
0
0.05
0.10
0.15
0.20
0.25
0.30
0.25
TEMPERATURE DIFFERENCE, °C
0
5
10
15
20
25
30

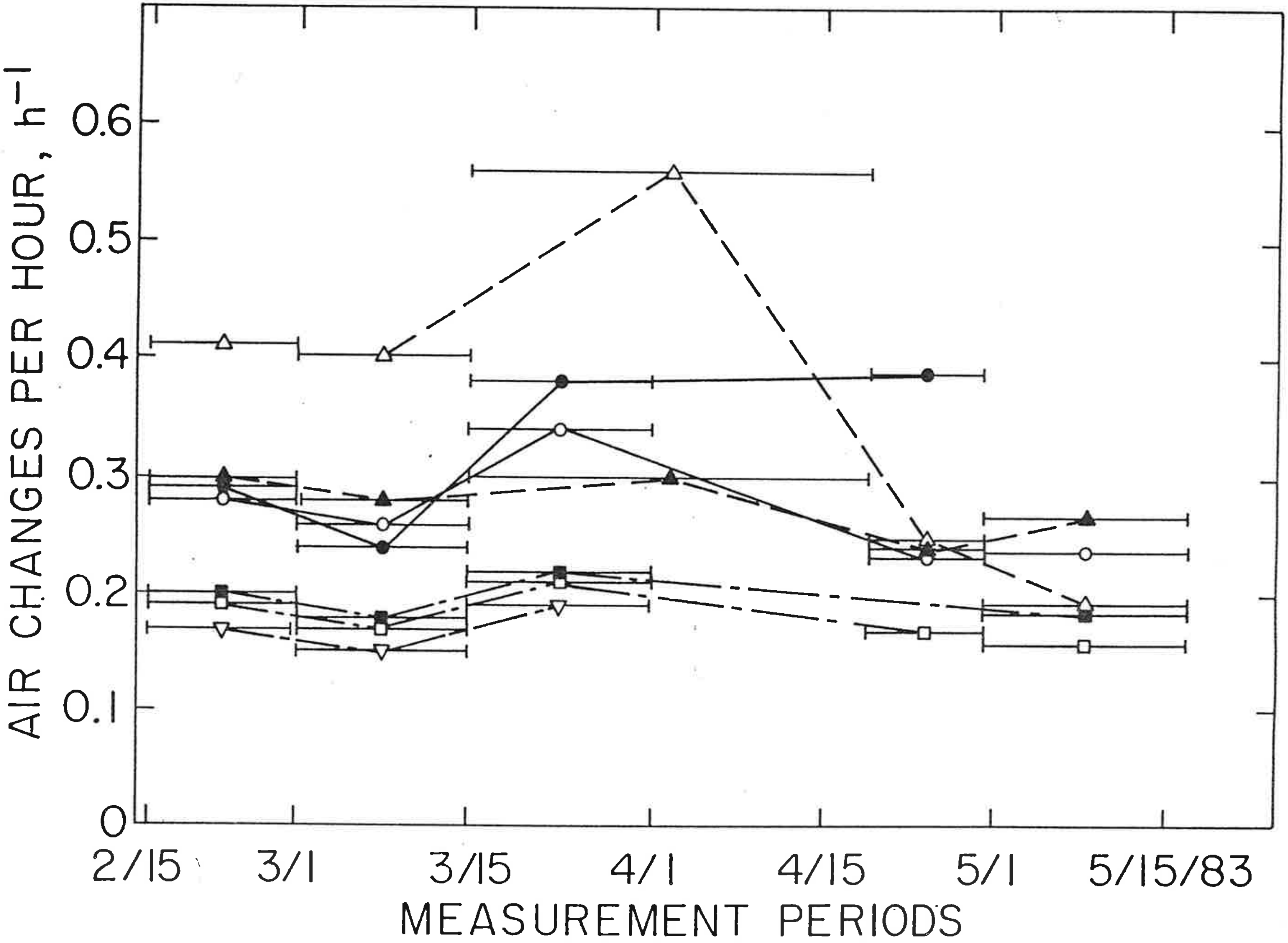
AIR CHANGES PER HOUR, h^{-1}
0.6
0.5
0.4
0.3
0.2
0.1
0
2/15
3/1
3/15
4/1
4/15
5/1
5/15/83
MEASUREMENT PERIODS

Fig. 12

3 Zone

Attic — Living Area — Crawl Space

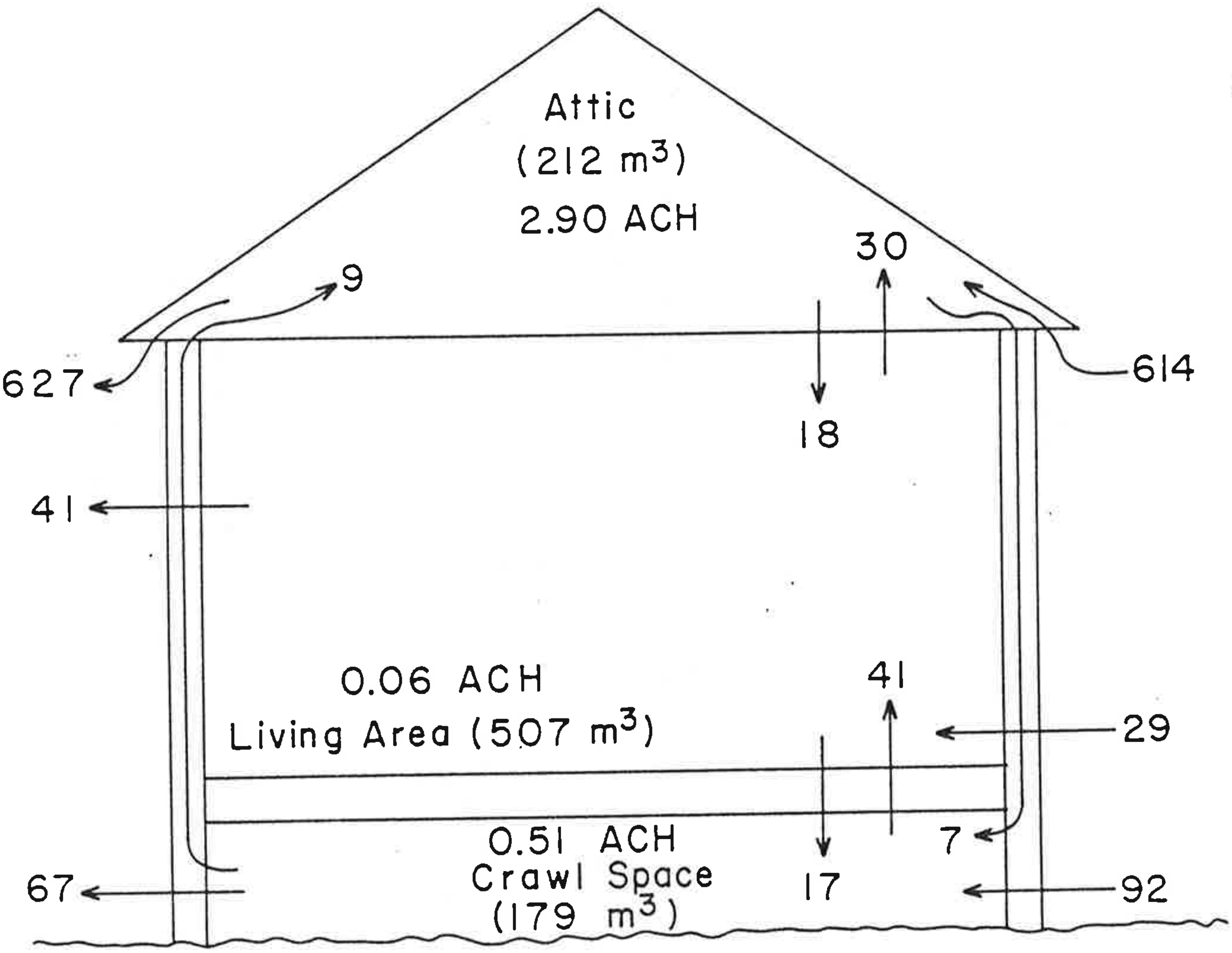

ILLINOIS HOUSE

(All Flow Rates in m^3/h)

Fig. 13

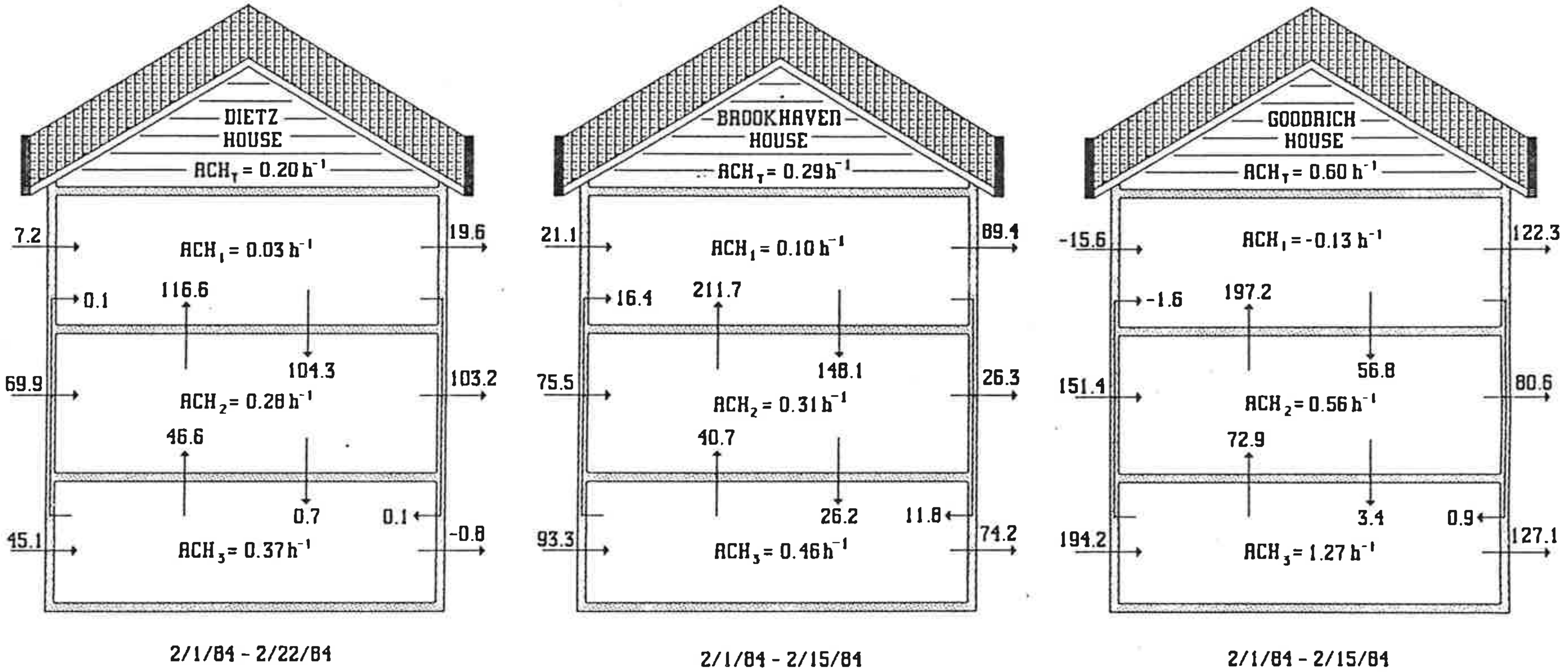
DIETZ HOUSE
$ACH_T = 0.20\,h^{-1}$
$ACH_1 = 0.03\,h^{-1}$
$ACH_2 = 0.28\,h^{-1}$
$ACH_3 = 0.37\,h^{-1}$
7.2
19.6
0.1
116.6
104.3
69.9
103.2
46.6
0.7
0.1
-0.8
45.1
2/1/84 - 2/22/84
BROOKHAVEN HOUSE
$ACH_T = 0.29\,h^{-1}$
$ACH_1 = 0.10\,h^{-1}$
$ACH_2 = 0.31\,h^{-1}$
$ACH_3 = 0.46\,h^{-1}$
21.1
89.4
16.4
211.7
148.1
75.5
26.3
40.7
26.2
11.8
74.2
93.3
2/1/84 - 2/15/84
GOODRICH HOUSE
$ACH_T = 0.60\,h^{-1}$
$ACH_1 = -0.13\,h^{-1}$
$ACH_2 = 0.56\,h^{-1}$
$ACH_3 = 1.27\,h^{-1}$
-15.6
122.3
-1.6
197.2
56.8
151.4
80.6
72.9
3.4
0.9
127.1
194.2
2/1/84 - 2/15/84

Fig. 14

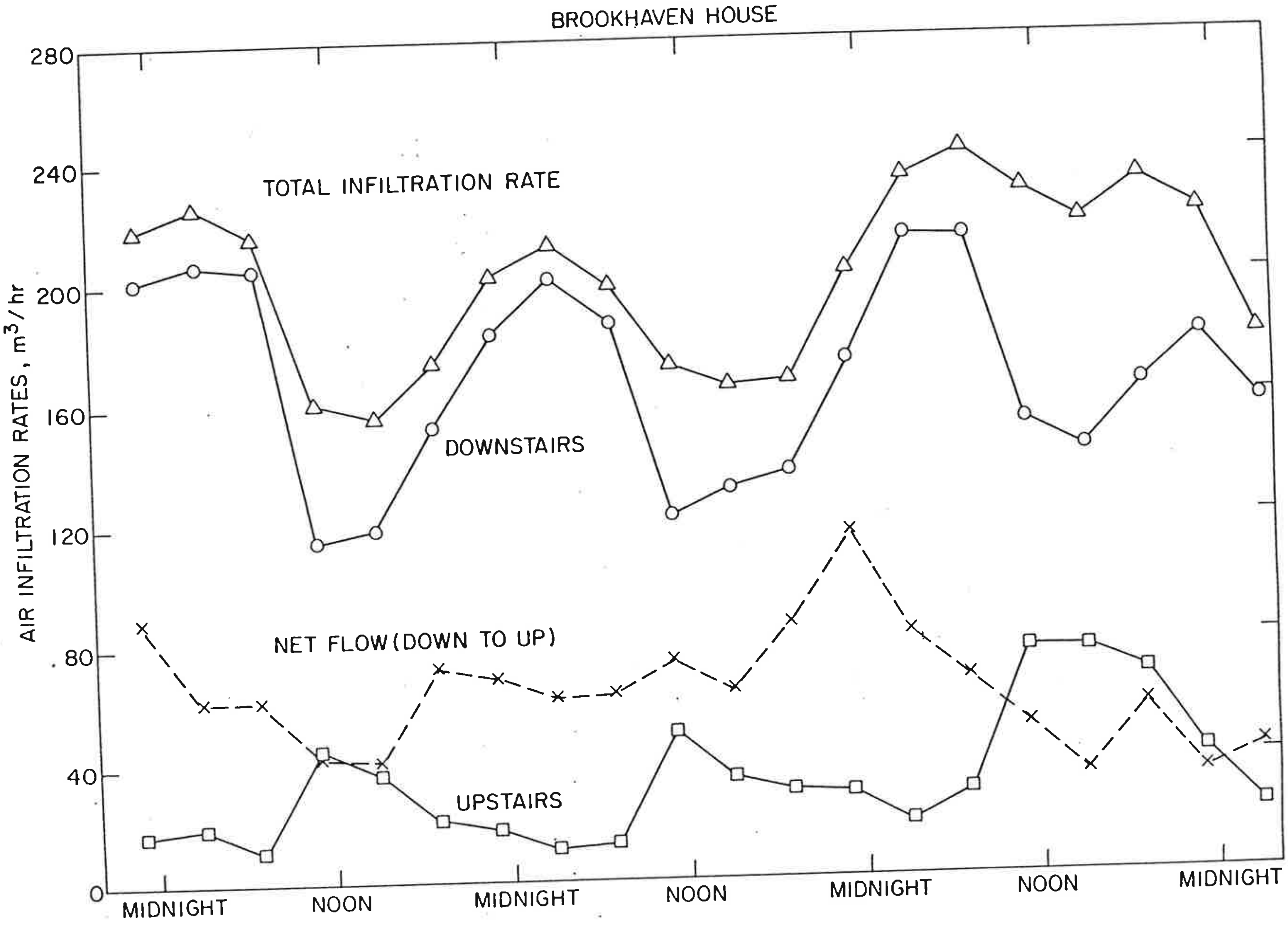
BROOKHAVEN HOUSE
TOTAL INFILTRATION RATE
DOWNSTAIRS
NET FLOW (DOWN TO UP)
UPSTAIRS
AIR INFILTRATION RATES, m^3/hr
0
40
80
120
160
200
240
280
MIDNIGHT
NOON
MIDNIGHT
NOON
MIDNIGHT
NOON
MIDNIGHT

Fig. 15

APPENDIX 1

The solution to the 2- and 3-zone infiltration models are provided in this appendix.

Two-Zone Case

$$R_{21} = \frac{R_{s1}\ C_{21}}{C_{11}\ C_{22} - C_{12}\ C_{21}}$$

$$R_{12} = \frac{R_{s2}\ C_{12}}{C_{11}\ C_{22} - C_{12}\ C_{21}}$$

$$R_{E1} = R_{21}\ \frac{C_{22}}{C_{21}} - R_{12}$$

$$R_{E2} = R_{12}\ \frac{C_{11}}{C_{12}} - R_{21}$$

R_{I1} and R_{I2} are calculated from Eqs 8 and 9 in the text.

Three-Zone Case

Let

$$[\quad] = [C_{11}(C_{22}\ C_{33} - C_{23}\ C_{32}) + C_{12}\ (C_{23}\ C_{31} - C_{21}\ C_{33}) + C_{13}\ (C_{21}\ C_{32} - C_{22}\ C_{31})]$$

Then

$$R_{21} = R_{s1}\ (C_{21}\ C_{33} - C_{23}\ C_{31})/[\quad]$$

$$R_{31} = R_{s1}\ (C_{22}\ C_{31} - C_{21}\ C_{32})/[\quad]$$

$$R_{32} = R_{s2}\ (C_{11}\ C_{32} - C_{12}\ C_{31})/[\quad]$$

$$R_{12} = R_{s2}\ (C_{12}\ C_{33} - C_{13}\ C_{32})/[\quad]$$

$$R_{13} = R_{s3}\ (C_{13}\ C_{22} - C_{12}\ C_{23})/[\qquad]$$

$$R_{23} = R_{s3}\ (C_{23}\ C_{11} - C_{13}\ C_{21})/[\qquad]$$

$$R_{E1} = R_{31}\frac{C_{23}}{C_{21}} + R_{21}\frac{C_{22}}{C_{21}} - R_{13} - R_{12}$$

$$R_{E2} = R_{32}\frac{C_{13}}{C_{12}} + R_{12}\frac{C_{11}}{C_{12}} - R_{23} - R_{21}$$

$$R_{E3} = R_{13}\frac{C_{11}}{C_{13}} + R_{23}\frac{C_{12}}{C_{13}} - R_{31} - R_{32}$$

$$R_{I1} = R_{E1} + R_{12} + R_{13} - R_{21} - R_{31}$$

$$R_{I2} = R_{E2} + R_{21} + R_{23} - R_{12} - R_{32}$$

$$R_{I3} = R_{E3} + R_{31} + R_{32} - R_{13} - R_{23}$$

The total air change per hour in a house is given simply by the sum of the exfiltration rates of all zones divided by the sum of the volume of all zones. (See p. 20 of the text for definition of the terms.)